Effects of Sodium Citrate on Slime Coatings in Bitumen Extraction

by

Dingfang Zhang

A thesis submitted in partial fulfillment of the requirements for the degree of

Master of Science

in

Chemical Engineering

Department of Chemical and Materials Engineering
University of Alberta

ABSTRACT

Albertan oil sands ores are becoming more difficult to process efficiently as the clay content of the ore increases and the grade of the ore worsens. A key to improving the extraction of bitumen from low-grade oil sands, thereby increasing the longevity of this critical resource, is reducing the formation of slime coating. Slime coating, which refers to the coverage of fine particles on the surface of bitumen droplets, can have a significant impact on the performance of flotation and hence on bitumen extraction recovery from oil sand ores.

Recently, addition of sodium citrate during the alkaline hot-water extraction process was shown to improve bitumen recovery and froth quality. Along with increased bitumen extraction efficiency, the addition of sodium citrate generated considerable environmental benefits, including less bitumen contained in tailings, more efficient water usage, and reduced energy intensity involved in the separation process.

The objective of the current study was to advance the fundamental understanding of the role sodium citrate has on reducing bitumen slime coating in the aeration stage of oil sands processing. Methods employed were zeta potential distribution measurements using Zetaphoremeter, the measurements of interactions between bitumen and clay particles using QCM-D in various model electrolyte solutions, and the analysis of calcium adsorption on montmorillonite particles using inductively coupled plasma (ICP) analysis. It was shown that sodium citrate can prevent slime coating from occurring, but sodium citrate cannot remove slime coating once it has occurred. Therefore, the addition of

sodium citrate at the beginning of the bitumen extraction process can lead to a more efficient and environmentally-friendly processing of a valuable energy resource.

ACKNOWLEDGMENTS

Firstly, I want to thank my supervisor, Dr. Qingxia Liu, for his excellent advice, generous support and encouragement during my MSc program, and for giving me the opportunity to participate in this project and work with such smart and hardworking people. I have learned a lot during this two-year program that will continue influencing me for a lifetime.

I am truly grateful to Dr. Jun Long and Syncrude Canada Ltd. for generously funding the project and providing helpful suggestions from an industrial perspective.

I would also like to express my gratitude to the support from many people in our group, especially Bailin Xiang and Dr. James Grundy. Without their help and fulfilling experience, it would have been impossible for me to complete all my experiments so quickly.

Much appreciation goes to Jim Skwarok, Ni Yang, and Shiraz Merali for their professional technical support and experienced instrument training throughout the whole process of my research.

Many thanks to all my family and friends for supporting me from both the spiritual aspect and material aspect. I am so grateful to my parents for their love throughout my whole life. Without their love and support, I could not become the person who I am right now. I will continue to work hard in the future and try my best to make them proud of me.

Table of Contents

List of Figures

NOMENCLATURE

Abbreviations

SPA	Secondary processing aid
SEM	Scanning electron microscopy
QCM-D	Quartz crystal microbalance with dissipation monitoring
T	Tetrahedron
O	Octahedron
ICP-MS	Inductively coupled plasma mass spectroscopy
AAS	Atomic absorption spectrometer
SAGD	Steam assisted gravity drainage
EOR	Inhanced oil recovery
CSS	Cyclic steam stimulation
HWGS	Hot water-based gravity separation process
LHES	Laboratory hydrotransport extraction system
AFM	Atomic force microscopy
vdW	Van der Waals
EDL	Electrostatic double layer
DLVO	Derjaguin-Landau-Verwey-Overbeek

Symbols

ξ	Zeta potential
ΔG	Gibbs free energy
ΔA	Surface area

$\gamma_{S/W}$	Interfacial tension between sand grain and water
$\gamma_{B/W}$	Interfacial tension between bitumen and water
$\gamma_{B/S}$	Interfacial tension between bitumen and sand grain
$\gamma_{B/A}$	Interfacial tension between bitumen and air
$\gamma_{A/W}$	Interfacial tension between air and water
θ	Contact angle
d_{50}	Average particle size
Δf	Frequency response
ΔD	Dissipation response
n	Overtone number
f_0	Fundamental resonance frequency
$\rho_0, \rho_1, \rho_2, \rho_q$	Density
t_q	Thickness of the quartz crystal
C	Sensitivity constant
η_1, η_2, η_3	Viscosity
μ	Shear modulus
ω	Angular frequency of oscillation
h_0, h_1, h_2	Thickness

CHAPTER 1

1 Introduction and Objectives

1.1 Introduction

Oil sands, also known as tar sands or bituminous sands, are loose sand deposits containing highly viscous bitumen (Masliyah et al., 2004). In the Athabasca oil sands deposits, more than two million tonnes of oil sands ores are mined and processed daily (Alberta Energy Regulator, 2018). The oil sands from the Athabasca deposits contain approximately 6-14 wt% bitumen, 80-85 wt% mineral solids, and 5 wt% water (Strausz, 1989). The mineral solids are mostly composed of quartz silica sand with a small, varying amount of fines (<44 μm), which includes clays such as kaolinite, illite, and montmorillonite (Bichard, 1987).

Fines can interact with a number of species involved in the bitumen extraction process, especially bitumen droplets. When a small solid particle attaches to a bitumen droplet, it can become permanently attached to the bitumen droplet and prevent the bitumen droplet from directly contacting free air bubbles. It has been discovered that the processability of oil sands ores and bitumen extraction recovery both decrease with increasing fines content in the oil sands ores (Dang-Vu et al., 2009; Helpler & Smith, 1994). Therefore, preventing fines attachment during bitumen flotation can greatly improve flotation efficiency and overall bitumen recovery (Liu et al, 2002).

Slime coating, a term commonly used in the mineral processing industry to describe the coverage of valuable minerals with a layer of fines, is considered to have a

significant impact on the performance of flotation and hence on bitumen extraction recovery from oil sands ores (Liu et al., 2004b). When slime coating occurs, the attachment of solid particles to the bitumen droplets creates a steric barrier retarding the coagulation of bitumen droplets with air bubbles used for flotation. Additionally, particle-laden bitumen droplets degrade the froth quality by carrying undesired solids, which are detrimental to bitumen recovery and raise the difficulty of subsequent froth treatment (Gu et al., 2004).

To better understand the impact of fines on bitumen recovery, previous researchers tested oil sands ore processability under various operating conditions. It was observed that separate addition of either 1 mM calcium ions or 1 wt% clay (montmorillonite, kaolinite and illite) to oil sand ores had a marginal effect on bitumen flotation efficiency. Furthermore, the addition of 1 mM calcium ions along with 1 wt% kaolinite or illite during flotation only slightly depressed bitumen recovery (Liu et al., 2002; Ding et al., 2008). However, bitumen recovery decreased sharply when both 1 mM calcium and 1 wt% montmorillonite clay were added to oil sands ores, indicating a detrimental effect of the combination of calcium ions and montmorillonite clay (Kasongo et al., 2000); similar effects have also been demonstrated for flotation of coal (Arnold & Aplan, 1986). The presence of calcium ions can activate the strong attraction between montmorillonite clay particles and bitumen droplets, leading to the slime coating of montmorillonite clay on the bitumen surface (Liu et al, 2004a).

The presence of montmorillonite, kaolinite or illite clay particles on bitumen droplet surfaces made it challenging for both bitumen-air bubble attachment and bitumen-

bitumen coalescence, leading to low bitumen flotation efficiency and depressed bitumen recovery. The proposed mechanism of slime coating is a reduction of electric double layer forces and formation of a cation linker in the presence of divalent cations, resulting in clay deposition on bitumen (Liu et al., 2004a; Long et al., 2006). Thus, a desirable chemical processing aid is demanded that can diminish the effect of calcium ions or other metal cations on slime coating while not impact the overall extraction performance.

Recently, the effectiveness of sodium citrate as a secondary processing aid (SPA) on the extraction process has been tested by Syncrude, Canada Ltd. It was discovered that, especially for lower grade ores, both bitumen recovery and froth quality could be dramatically improved by adding sodium citrate or a combination of sodium citrate and caustic (NaOH) to condition the oil sand slurry. This combination also generated considerable environmental benefits, including less bitumen remaining in tailings, more efficient water usage, and reduced energy intensity involved in the separation process (US Patent No. US 2015/0210929 A1, 2015).

Sodium citrate is widely used as a preservative in foods, an acidity regulator which can resist changes in pH, and a chelating agent that binds strongly to metal cations, making it an excellent secondary process chemical aid with caustic (US Patent No. US 2015/0210929 A1, 2015). Although it has been shown that sodium hydroxide combined with sodium citrate significantly boosts the bitumen extraction efficiency of mined oil sands, the critical roles citrate play in the liberation and aeration stages still need to be investigated.

1.2 Research Objectives

The objective of the current study was to advance the understanding of the effects of sodium citrate on bitumen slime coating in the aeration stage in bitumen extraction. The detrimental impact of montmorillonite clay has already been verified by J. Liu at the University of Alberta (Liu et al., 2002), particularly in the presence of divalent cations. Accordingly, the current study mainly focused on whether sodium citrate could prevent montmorillonite from forming a slime coating and whether sodium citrate could remove slime coating once formed. Additionally, since the dominant clay mineral commonly encountered in the Athabasca oil sands ore is kaolinite, the impact of sodium citrate on slime coating caused by kaolinite was also investigated. To achieve these objectives, a Zetaphoremeter was used to study the effect of sodium citrate on the zeta potentials of bitumen, clay particles, and mixtures of bitumen and clay in the presence and absence of calcium ions. Additionally, a quartz crystal microbalance with dissipation monitoring (QCM-D) was used to measure the interactions between bitumen, clay particles, and their mixture with and without the addition of sodium citrate and calcium to further confirm the results from zeta potential distribution measurements. Lastly, a batch adsorption study of calcium onto montmorillonite in the presence of sodium citrate elucidated the mechanism by which citrate reduces slime coatings. The mechanistic understanding of sodium citrate for improving bitumen extraction not only helps the industry to improve extraction efficiency, it also guides the industry to potentially discover a more efficient SPA to improve recovery for both good and poor ores.

1.3 Thesis Outline

This thesis is organized as follows:

Chapter 1

- Briefly introduces the overview of bitumen extraction from Athabasca oil sands in Canada. Moreover, the problem of slime coating in the extraction process is identified. A solution to this problem is proposed—using sodium citrate as a secondary processing aid.

Chapter 2

- Provides a summary of the literature related to the oil sands and the principles of colloidal and clay science.

Chapter 3

- Presents zeta potential distribution measurement for studying the effects of sodium citrate on the surface potentials of bitumen droplets and clay particles, including the materials, the principle of the technique, measurement procedures, results and discussion.

Chapter 4

- Presents QCM-D measurement for investigating the impact of sodium citrate on the interactions between bitumen droplets and clay particles, including the materials, the principle of the technique, measurement procedures, results and discussion.

Chapter 5

- Studies the role of sodium citrate in the adsorption of calcium ions on montmorillonite clay particles investigated by batch adsorption experiments and

aqueous inductively coupled plasma mass spectrometry (ICP-MS), including the materials, sample preparation procedure, results and discussion.

Chapter 6

- Summarizes the conclusions obtained from the experimental results and possible mechanisms. Future work is proposed to figure out the fundamental mechanism of slime coating and the effectiveness of sodium citrate on preventing bitumen-clay coagulation in process water or promoting bitumen-air coagulation under different conditions, such as in the presence of various divalent cations, different pH, and varying ionic strengths.

CHAPTER 2

2 Literature Review

2.1 Athabasca Oil Sands Area

Canada's oil sands reserves are mainly located in Alberta. They encompass an area of about 280,000 km^2 and contain more than 160 billion barrels of recoverable oil (Alberta Government, Summer 2018). Moreover, Alberta's deposit is the largest in the world that can be used to extract the very highly viscous bitumen. The Athabasca oil sands area is the largest oil sands deposit among the three deposits in Alberta, Canada; the other two are the Peace River and Cold Lake regions (Carrigy, 1974).

There are many hypotheses about the formation of oil sands. One of the most widely accepted is that hydrocarbons, formed from the decomposition of plankton and other marine animals millions of years ago, gradually degraded to light oil at appropriate temperatures and depths. As the Rocky Mountains formed, the light oil was transported toward the Saskatchewan border by oxygenated water. At the same time, the microbes in the water fed off the lighter hydrocarbon molecules, leaving behind heavier complex hydrocarbons that gradually formed the Albertan oil sands deposits (Hein et al., 2008).

2.2 Physical and Chemical Properties of Oil Sands

2.2.1 Oil Sands Composition

Alberta's oil sands typically consist of around 10% bitumen, 85% sands (including minerals and clays) and 5% water by mass, as shown in Fig. 2.1 (Takamura, 1982). Bitumen is classified as an extra heavy oil due to its high viscosity at room temperature and complex hydrocarbon composition; bitumen has an API gravity of around 8° at room temperature, meaning it is denser than water. Oil sands are usually classified as good, average and poor processing ores depending on the content of bitumen and fines of the oil sands ores (Banerjee, 2012). The mineral solids in oil sands mostly consist of quartz or silica sand. Particles with size >44 μm are defined as coarse, while those with size <44 μm are defined as fines. Oil sands deposits with high fines content and lower bitumen grade are generally considered to be poor ores.

A thin layer of water, located between the quartz and bitumen, makes the oil sands water-wet, which enables the extraction of bitumen from oil sands by using a hot-water extraction technique. Water in the oil sands normally contains various soluble ions, such as sodium, potassium, calcium, chloride and sulphate, some of which can be detrimental to the bitumen extraction process. The properties of oil sands play a significant role in determining the processability of oil sands ores and also impact the choices of operation conditions and types of equipment used during the extraction process (Hepler & Smith, 1994).

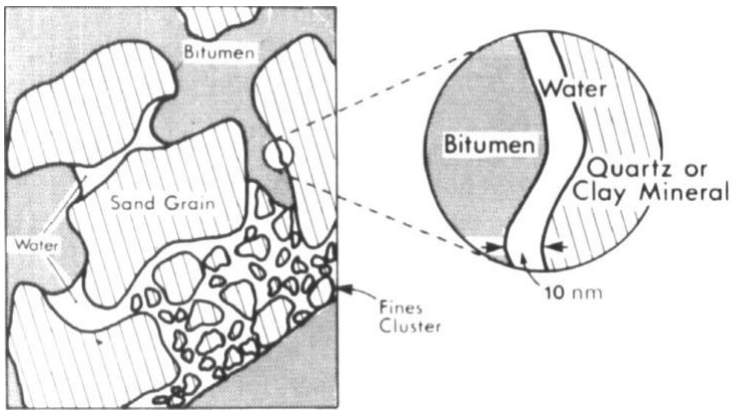

Figure 2.1 Oil sands composition in Athabasca, Canada, proposed by Takamura (Takamura, 1982). Reprinted with permission from John Wiley & Sons, Inc.

2.2.2 Clay Minerals

Clays are generally considered fines of <2 μm in size, but the particle size distribution of clay minerals can vary dramatically from submicron-size to over 1 mm (Bichard, 1987). The clay distribution in oil sands typically consists of 69% kaolinite, 28% illite, 1.7% mixed-layer clay, 1% chlorite and 0.3% smectite. These clay minerals have a flat, plate-like shape and contain two basic layers, as shown in Fig. 2.2: a silicon-oxygen tetrahedron sheet (T) and an aluminum-oxygen-hydroxyl octahedron sheet (O) (Konan et al., 2007). Arrangements of these two basic sheets lead to particular types of clay minerals with different properties. For example, kaolinite has a two-layer O-T structure while illite and montmorillonite both have a three-layer T-O-T structure (Bergaya & Lagaly, 2006). The T and O sheets are usually electrically neutral, but isomorphic substitution of higher valance cations by low valence cations of similar sizes can result in a net charge deficiency on the sheet surface and cause the whole clay particle to be negatively charged. To balance the charge deficiency, compensating

cations, such as calcium ions, are attracted to the negative charges and make the clay minerals electrically neutral again. Therefore, isomorphic substitution and the location of compensating ions contribute greatly to the electric surface properties of clay minerals (Dékány, 2002). For example, in 1:1 (T:O) kaolinite, the isomorphic substitution of Al^{3+} for Si^{4+} is low and mainly occurs in the tetrahedron sheets, causing relatively low cationic exchangeability. However, for 2:1-type (T:O) montmorillonite, isomorphic substitution occurs in both the tetrahedron and octahedron sheets, leading to a higher cation exchange capacity than kaolinite. The degree of isomorphic substitution and layer structure type significantly affect the zeta potential of clay. In process water, which contains calcium ions, calcium ions can be taken up by the clays, which is detrimental to the bitumen extraction process.

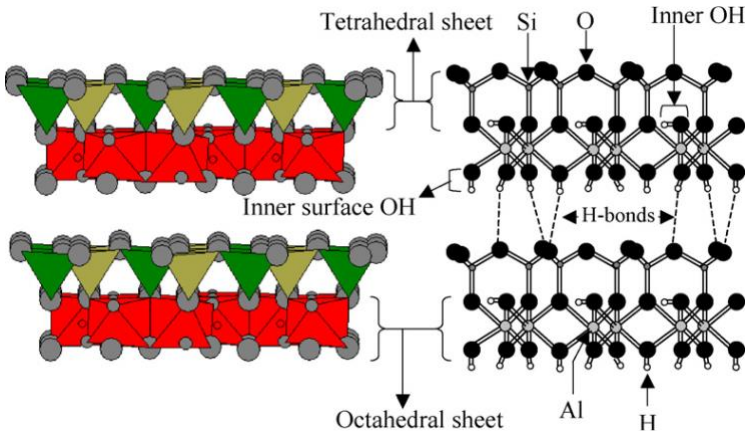

Figure 2.2 Clay layers: silicon-oxygen tetrahedron sheet (T) and an aluminum-oxygen-hydroxyl octahedron sheet (O) as depicted by Konan et al. (2007). Reprinted with permission from Elsevier.

2.3 Oil Sands Processing

There are two commonly-used methods to extract bitumen depending on the depth of the oil sands deposit below the surface: in-situ production and open-pit mining (Vashishtha & Maheshwari, 2014). In-situ production is applied when the depth is greater than 75 m underground, which is too deep for mining. Most of the oil sands reserves are recoverable using the in-situ method, and roughly half of Canadian bitumen is currently extracted using in-situ methods (Masliyah et al., 2011). The leading three technologies known as in-situ methods are steam assisted gravity drainage (SAGD), enhanced oil recovery (EOR), and cyclic steam stimulation (CSS).

The bitumen and solids in Athabasca oil sands are coated with a layer of water, which enables the separation of the bitumen from the sands using hot water-based gravity separation process (HWGS) (Dai & Chung, 1995). This widely-used process for extraction of bitumen from mined oil sands is exhibited in Fig. 2.3. Firstly, the oil sands ores are crushed and mixed with water and additives to prepare slurries either in rotary breakers, cyclo-feeders or mixing boxes. Then the slurry is conditioned with warm process water, processing aids and air, and fed into hydrotransport pipelines. Bitumen is liberated from the sand grains during transport through these pipelines. The whole bitumen liberation process can be divided into two separate parts: bitumen recession on the sand grains and bitumen separation from sand grains, as shown in Fig. 2.4. The liberated hydrophobic bitumen droplets can attach to free air bubbles, a process known as bitumen aeration, as exhibited in Fig. 2.4. Since the aerated bitumen froth is relatively light, it will float to the top of the gravity separation vessel. At the

same time, the heavier coarse particles remaining in the slurry will automatically sink to the bottom of the separation vessel. The middlings that neither float nor sink and contain fine solids, clays and free bitumen are fed into flotation cells for further bitumen recovery. The composition of the bitumen froth recovered from the aeration stage usually is 60 wt% bitumen, 30 wt% water and 10 wt% solids. The bitumen froth is first deaerated and then fed into the bitumen froth treatment plant to remove solids and water. Finally, the recovered bitumen is upgraded and sent to refineries. The slurries that remain after flotation are diverted to tailing ponds or recycled back to the front of the processing plant (Das & Butler, 1998; Dai & Chung, 1996).

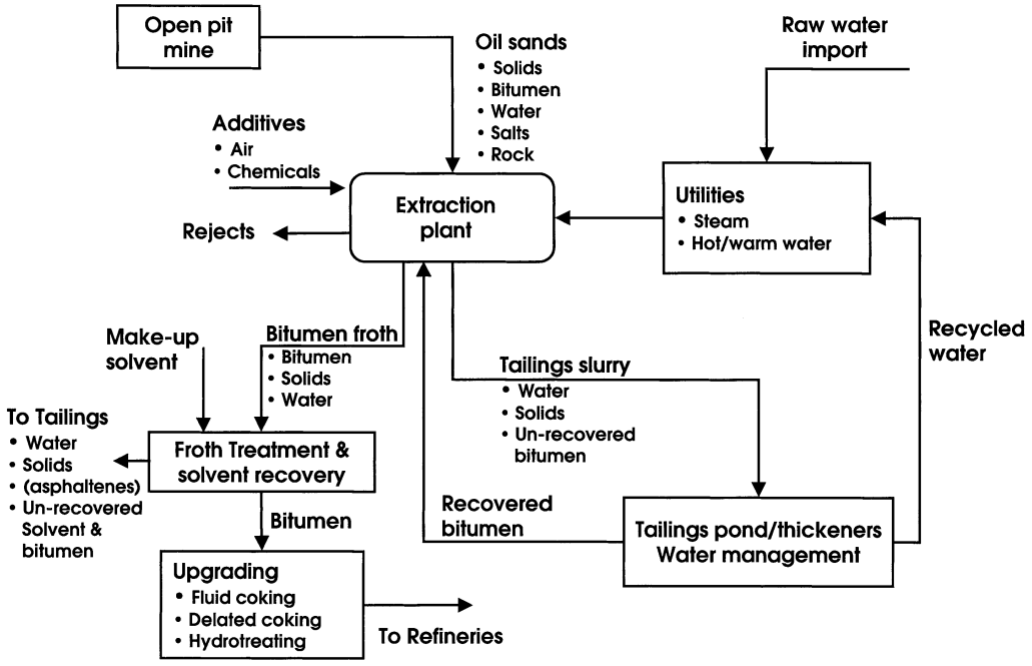

Figure 2.3 Schematic unit operations of the bitumen extraction process using water-based extraction processes (Masliyah et al., 2004). Reprinted with permission from John Wiley & Sons, Inc.

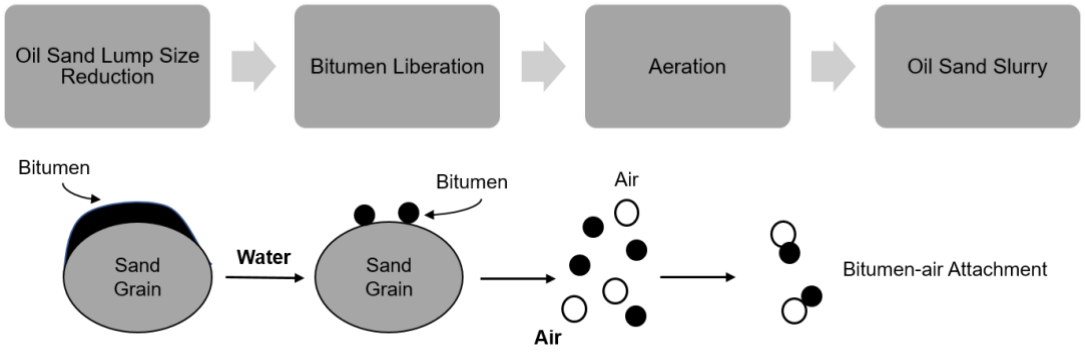

Figure 2.4 Schematic diagram of bitumen liberation and aeration stage.

2.3.1 Bitumen Liberation

The bitumen liberation process can be divided into two steps: first, bitumen recesses on the grain sands in water; second, bitumen droplets separate or detach from the sand grains in water. It has been shown that clay addition has a marginal effect on bitumen detachment, indicating that high clay-content ores decrease bitumen recovery by affecting bitumen aeration, not liberation (Basu et al., 1998).

During the bitumen liberation process, as shown in Fig. 2.5, the interfacial energy change is given by Eq. 2.1 (Masliyah et al., 2011).

$$\frac{\Delta G}{\Delta A} = \gamma_{S/W} + \gamma_{B/W} - \gamma_{B/S} \tag{2.1}$$

In this equation, ΔG is the change in interfacial energy, ΔA is the change in interfacial area, and $\gamma_{S/W}$, $\gamma_{B/W}$, and $\gamma_{B/S}$ are the interfacial tensions of the sand grain-water, bitumen-water, and bitumen-sand grain interfaces, respectively. Although the values of interfacial tension of sand-water and bitumen-sand cannot be measured directly, the difference between them can be derived from Young's equation (Eq. 2.2).

$$\gamma_{B/S} - \gamma_{S/W} = \gamma_{B/W} \cos\theta \quad (2.2)$$

By inserting Eq. 2.2 into Eq. 2.1, it is shown that

$$\frac{\Delta G}{\Delta A} = \gamma_{B/W}(1 - \cos\theta) \quad (2.3)$$

From Eq. 2.3, it can be noted that bitumen can detach from sand grains only under the condition when the contact angle of bitumen on sand grain is equal to 0°, which indicates that sand grains must be completely hydrophilic. Therefore, bitumen detachment from sand grains is thermodynamically unfavourable, and other mechanical energies (e.g., hydrodynamic forces) are required (Basu et al., 1997). Since $\gamma_{B/S}$ cannot be easily changed, $\gamma_{S/W}$ is reduced to improve bitumen liberation by increasing pH, as high pH makes the sand surface more negatively charged and more hydrophilic.

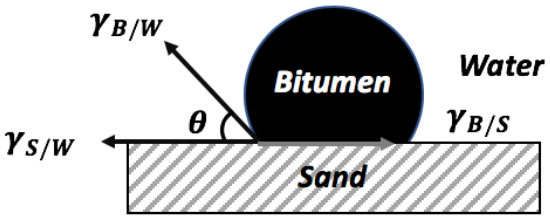

Figure 2.5 The equilibrium contact angle (θ) of bitumen on sand grain.

A significant number of methods have been developed to investigate factors affecting the bitumen liberation process, such as temperature, pH, and clay addition. Basu et al. (1997) first tested the effect of pH on the bitumen film thinning and film rupture process by coating a thin circular bitumen film on a microscope glass slide. A laboratory hydrotransport extraction system (LHES) was developed to evaluate the

degree of bitumen liberation by Wallwork et al. (2004). The different colours exhibited by bitumen-covered sand grains and clean sand grains allowed determination of the degree of liberation by analyzing the darkness of sand grains images captured by CCD camera. It was discovered that low operating temperature decreased bitumen liberation efficiency, while air addition had a positive effect on bitumen recovery for both poor ores and good ores. The atomic force microscope (AFM) was also used to investigate bitumen-sand interactions under different conditions. Zhao et al. (2006) studied the interactions of bitumen and sand grains with the addition of divalent cations, surfactants, and their combinations. They found that divalent cations decreased bitumen liberation due to an increased adhesion force and decreased long-range repulsive forces between bitumen and silica. Conversely, the addition of surfactant decreased the adhesion force, showing they can be used to alleviate the detrimental effect of divalent cations on bitumen recovery (Zhao et al., 2006). Xiang et al. (2018) investigated the effects of solid wettability, solution pH and operation temperature on the bitumen liberation process using a QCM-D. By recording the frequency and dissipation responses of the bitumen-coated silica sensor, the bitumen detachment process was analyzed quantitively. High solution pH and increasing temperature can enhance the degree of bitumen liberation greatly, and detachment of bitumen from a hydrophobic solid surface was more difficult under the normal bitumen extraction process conditions. Additionally, adding citrate as a SPA was found to increase the kinetics of bitumen liberation.

2.3.2 Bitumen Aeration

Bitumen aeration, defined as the attachment of bitumen droplets to air bubbles, is another critical step in the bitumen extraction process. If bitumen droplets are not aerated after liberation from sand grains, they will remain in the slurry due to the similar density with water. The attachment of air bubbles to bitumen droplets results in an air-bitumen floc with a density lower than water, that floats to the top of the slurry in the separation vessel where it is recovered as a froth. The free energy change during the aeration process is given by Eq. 2.4, where $\frac{\Delta G}{\Delta A}$ represents the specific energy change, A represents air bubble, B represents bitumen, and W represents water (Masliyah et al., 2011).

$$\frac{\Delta G}{\Delta A} = \gamma_{B/A} - (\gamma_{B/W} + \gamma_{A/W}) \tag{2.4}$$

Young's equation associated with this process is given by Eq. 2.5.

$$\gamma_{B/A} - \gamma_{B/W} = \gamma_{A/W} \cos\theta \tag{2.5}$$

By inserting Eq. 2.5 into Eq. 2.4, it leads to

$$\frac{\Delta G}{\Delta A} = \gamma_{A/W}(\cos\theta - 1) \tag{2.6}$$

It can be noted that $\frac{\Delta G}{\Delta A} \leq 0$ because $\cos\theta \leq 1$, suggesting that the attachment of air bubbles to bitumen is thermodynamically spontaneous. The larger the contact angle, the more negative the free energy change will be and more favourable it will be for the bitumen attachment to air bubbles.

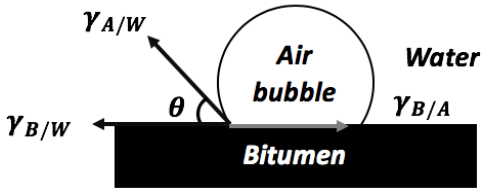

Figure 2.6 The equilibrium water contact angle (θ) of an air bubble on bitumen.

The bitumen aeration process has been studied using various techniques. Moran et al. (2000) studied the factors affecting the attachment of bitumen droplets to air bubbles using a micromechanical method. They found that bitumen aeration could be promoted with smaller-sized bitumen droplets and higher aqueous phase ionic strength, as higher ionic strength would decrease the repulsive electric double layer force. On the other hand, the presence of fines can decrease the bitumen aeration efficiency because of the steric barrier preventing bitumen droplets from contacting air bubbles. The induction time measurement is another quantitative method to investigate the bitumen aeration process. This technique captures the interaction between gas bubbles and bitumen droplets with a high-speed digital imaging system. From the captured images, the time of bitumen-bubble interaction before attachment is found (Gu et al., 2004). Different factors, such as temperature, bubble size, bubble impact velocity, and the presence of surfactants and dissolved gases were examined by Najafi et al. (2008) to observe their effects on bitumen-air bubble attachment.

2.3.3 Role of pH in Bitumen Extraction

Processing aids are added to enhance bitumen recovery in oil sands industry, and the most widely used ones are sodium hydroxide, surfactants and polymers (Flury et al., 2013; Schramm, 2000; Li et al., 2008). Although using sodium hydroxide as a processing aid cannot obtain the highest bitumen recovery, it is the best option in the oil sands industry due to the lower cost and good performance. As an activating agent, sodium hydroxide can cause the release of surfactants from the bitumen surface. The increased pH and released surfactants can change the surface properties of bitumen, sand grains and other components, which all influence the bitumen extraction efficiency.

By considering the favourable pH for both bitumen aeration (low pH) and liberation (high pH), it is concluded that it is vital to control the pH within a moderate range that can be beneficial to both processes. The role of pH in the bitumen extraction process has been studied by Bakhtiari et al. (2015). He showed that the surfaces of bitumen and sand grains are more negatively charged at alkaline pH. The negatively-charged surfaces promoted the repulsive interactions between bitumen and sand grains, resulting in higher bitumen liberation efficiency. The same conclusion has been proved by other techniques.

However, increasing the pH is not beneficial for bitumen aeration step, as the bitumen surface would become more negatively charged and less hydrophobic due to the adsorption of released surfactants on bitumen surface at alkaline pH. Gu, et al. (2003) found that the attachment time of bitumen to air bubbles increased with the addition

of sodium hydroxide to oil sands ore. Besides, bitumen coalescence plays a critical role in the bitumen extraction process. It was shown that bitumen droplets with a size larger than 1 mm could lead to the highest recovery (Wik et al., 2008). Liu et al. (2005a) used AFM to investigate the interactions between bitumen surfaces and found that both electrical double layer forces and hydrophobic forces are dominant forces involved in bitumen-bitumen coalescence. The increase of pH can lead to a stronger repulsive force and a weaker adhesion force, which prevents bitumen-bitumen coalescence and results in low bitumen recovery.

2.4 Slime Coating

Slime coating refers to the coverage of bitumen droplets with a layer of fine clays, which is considered to have a significant impact on the performance of flotation and hence on bitumen extraction recovery from oil sands ores (Wallace et al., 1989). If slime coating occurs in the bitumen extraction process, the attachment of solid particles to the bitumen droplet would not only set up a steric barrier retarding the contact of bitumen droplets with air bubbles, but it also degrades the froth quality by carrying undesired solids and raises the difficulty of subsequent froth treatment. The effects of calcium dosage and clay content on the bitumen extraction process have been examined by Kasongo et al. (2000). It was observed that the addition of 1 mM calcium ions or 1 wt% clay (montmorillonite, kaolinite or illite) separately or 1 mM calcium ions in combination with 1 wt% kaolinite or 1 wt% illite had a slight effect on bitumen recovery. However, bitumen recovery decreased sharply when 1 wt%

montmorillonite clay and 1 mM calcium ions were added to the oil sands ores, which suggested a detrimental synergistic effect of calcium ions with montmorillonite clay (Wallace et al., 1989).

Slime coating of bitumen by montmorillonite clay has been shown to have a negative impact on bitumen coalescence, as montmorillonite would raise the repulsion forces and diminish the adhesion forces between bitumen droplets (Liu et al., 2005). Liu et al. (2004a) discovered that the presence of calcium ions activated the strong attachment between montmorillonite clay and bitumen, leading to the slime coating of montmorillonite clay particles on the bitumen surface. It was proposed that calcium ions may attach to the negatively-charged clay particle surface and work as a "linker" between bitumen droplets and clay particles, but more research is required to prove this hypothesis.

Liu et al. (2002) developed a novel method to study the interactions of clays and bitumen based on zeta potential distributions. According to the distributions of a bitumen-clay mixture, the strength of interaction between bitumen and clay particles can be observed. This method works when the zeta potentials of the two components are significantly different, such as some clays and bitumen, but it cannot be used for two components with similar zeta potentials.

Recently, a QCM-D method was shown to be a promising way to examine bitumen-clay interactions under various pH values by Bakhtiari et al. (2015). A thin bitumen layer was coated on a silicon sensor, and a 1 wt% montmorillonite or kaolinite clay suspension under different aqueous conditions was pumped onto the sensor surface.

Based on the frequency and dissipation responses of the sensor, the deposition of clay particles on bitumen was analyzed quantitively.

Gan & Liu (2008) conducted experiments to investigate the impact of metal cations and citrate on the heterocoagulation of bitumen and kaolinite. At operating pH values, divalent metal cations enhanced heterocoagulation, while simultaneous addition of citrate significantly reduced the degree of the coagulation. They hypothesized that either the formation of metal-citrate complexes or the adsorption of citrate anions to the bitumen and kaolinite surfaces was responsible for the reduced activity of divalent metal cations.

In conclusion, the presence of clay particles on bitumen droplet surfaces reduces bitumen-air bubble attachment and bitumen-bitumen coalescence, which could also explain the low efficiency of bitumen flotation and depressed bitumen recovery. Therefore, it is desirable to find a processing aid to minimize the effect of calcium ions or other cations on slime coating while not impacting the overall extraction performance.

2.5 Surface Force

In colloidal systems, the solid and the contacting solution must remain electrically neutral. When the solid is negatively charged, the aqueous phase must have an equal but opposite charge. The electrical double layer consists of the charges on the surface, oppositely-charged ions immediately adjacent to the charged surface (the Stern layer), and an extended film of free ions with an elevated concentration of counterions called

diffuse layer (Schramm, 2006). Thus, a colloidal particle will exhibit a net charge, which is the charge at a surface close to the solid surface such that the aqueous phase within the surface is stationary upon movement of the particle, as shown in Fig. 2.7. This plane is called the slipping plane, and the potential at this surface is called the zeta potential, or ξ-potential. The electrical charge or potential of the particles directly and indirectly determines a great number of significant properties of colloidal systems. The potential distribution often determines the interaction energy between the particles and is responsible for the stability of particles towards coagulation. Many commercial instruments have been developed to measure zeta potentials by automatic measurements of electrophoretic mobility in the colloidal system and are widely used in the oil sands industry to understand the interactions between bitumen droplets and clay particles or air bubbles.

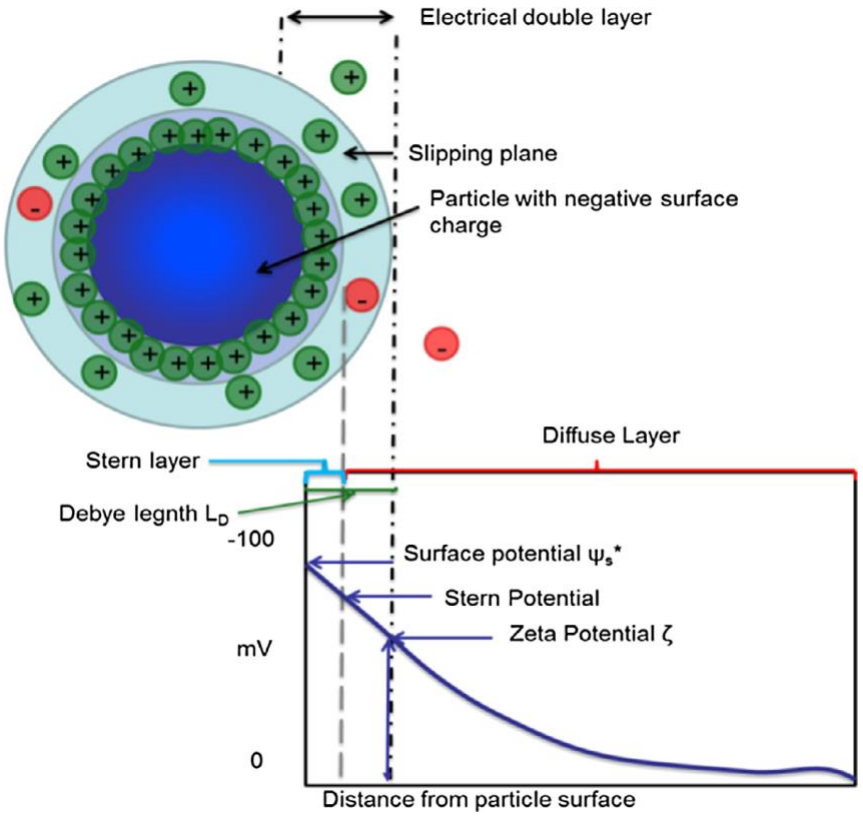

Figure 2.7 Electrical double layer (Valiño et al., 2014). Reprinted with permission from Elsevier.

The classical DLVO theory of colloidal interaction was first introduced by Derjaguin, Landau, Verwey and Overbeek, and it only considered van der Waals (vdW) and electrostatic double layer (EDL) forces between colloids. Classic DLVO maintains that the energy of a colloidal system is calculated as the sum of the vdW energy and the EDL energy (Butt & Kappl, 2010). However, DLVO theory is not capable of describing all colloidal phenomenon, such as the interactions for poor processing ores (Liu et al., 2004a). Hence, a more complex, extended DLVO theory was proposed that considered hydrophobic forces, hydration forces, repulsive steric forces, and attractive bridging forces. Liu et al. (2004a) discovered that the repulsive EDL force was the dominant

interaction between bitumen and silica for good processing ores, while both the EDL and hydrophobic forces played a significant role for bitumen-silica interaction in poor processing ores.

CHAPTER 3

3 Zeta Potential Distribution Measurement

3.1 Principles of the Technique

In the bitumen extraction process from mined oil sands, the electrokinetic behaviours of bitumen and fine clays substantially affect the bitumen liberation and aeration stages. Having a better understanding of the bitumen charging mechanisms would be quite helpful in solving issues related to bitumen extraction (Carrigy, 1974; Bowman, 1967).

When a particle is negatively charged, it attracts positive ions and repels negative ions in the aqueous media (Dékány, 2002). To quantify the strength of the charged particles, the electrophoretic mobility is determined experimentally. For most commercial instruments, it is common to measure the electrophoretic mobility of suspended particles or droplets and calculate the zeta potential using the Smoluchowski equation (Salopek et al., 1992). Zeta potential distribution measurement is a convincing and straightforward way to present the interactions between bitumen and clay in aqueous media. The approach of this application is illustrated below.

The zeta potential distributions of individual bitumen emulsion and clay suspensions usually are located at two distinct positions. When bitumen droplets and clay suspensions are mixed, the interactions between these two components can be inferred by comparing the zeta potential distribution of the mixture to the

distributions of the individual components, as illustrated in Fig. 3.1. For instance, if there is no interaction between the bitumen droplets and clay particles, two distinct distribution peaks would still be observed at positions near those measured for bitumen emulsion and clay suspension individually, as shown in Fig. 3.1b. On the other hand, if the clay particles readily attach to the bitumen droplet surface, the measured zeta potential distribution would exhibit only one peak whose position is determined by the clay to bitumen ratio. At a high clay to bitumen ratio, the bitumen droplets would be fully covered by the clay particles and a single peak would be located at the same zeta potential of individual clay suspensions, as shown in Fig. 3.1c. At a low clay to bitumen ratio, there would not be enough clay particles to ensure full surface coverage of all the bitumen droplet surfaces. In this case, the zeta potential of the bitumen/clay aggregate would be influenced by both the clay and bitumen zeta potentials, resulting in a single peak located in the middle of the original zeta potential distributions of bitumen emulsion and clay suspensions, as shown in Fig. 3.1d. Lastly, when clay is only weakly attracted to bitumen, not all the clay will attach to the bitumen droplets. Since two populations would exist in this scenario, free clay and bitumen/clay aggregates, two zeta potential peaks would be observed, as shown in Fig 3.1e. Like in Fig 3.1d, the position of the bitumen/clay aggregate peak depends on the fraction of bitumen surface that is covered by clay, which is a function of the ratio of clay to bitumen and the strength of attraction between bitumen droplets and clay particles. Thus, by observing the zeta potential distributions of aqueous bitumen/clay

mixtures in various electrolytes, the possibility and strength of slime coatings can be inferred.

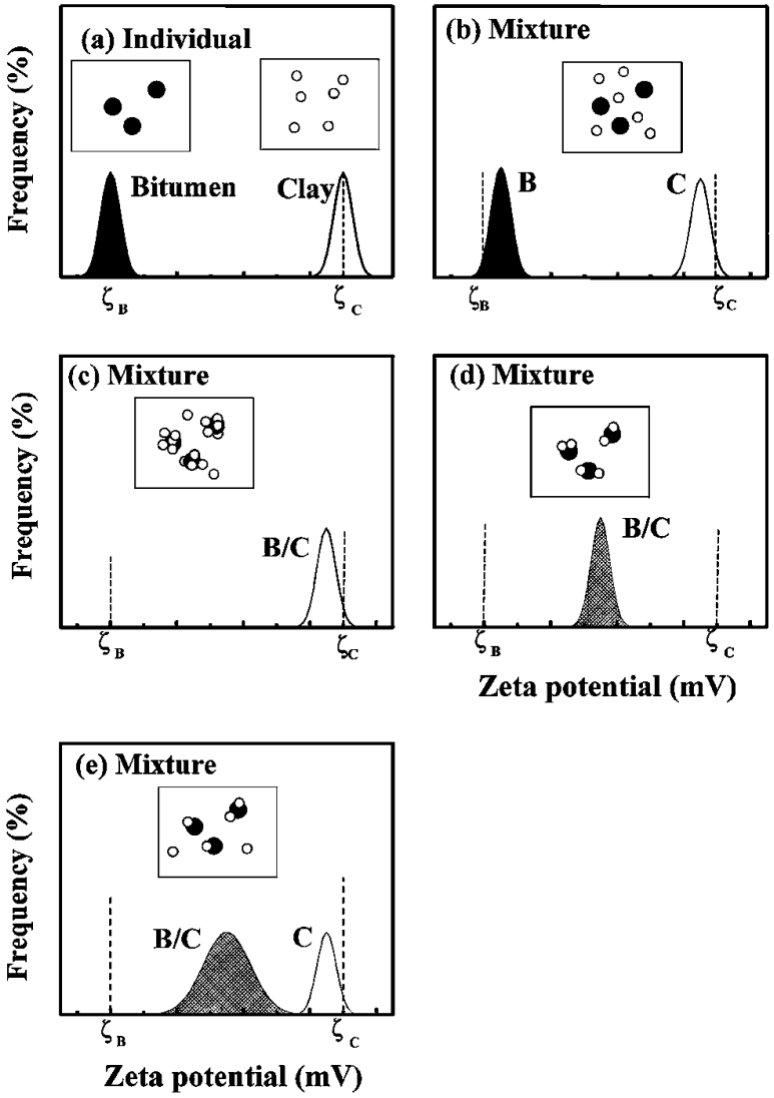

Figure 3.1 Zeta potential distributions of bitumen droplets and clay particles systems. Black particles and peaks represent bitumen droplets while white particles and peaks represent clay particles. Grey peaks indicate partially-covered bitumen droplets (Liu et al., 2002). Reprinted with permission from Elsevier.

3.2 Materials and Methods

3.2.1 Materials

Two types of clays, montmorillonite and kaolinite, were purchased from Ward's Science. Coker feed bitumen was provided by Syncrude Canada Ltd. Sodium citrate dihydrate (>99%, Sigma-Aldrich) was used as a secondary processing aid (SPA) and $CaCl_2 \cdot 2H_2O$ (ACS grade, Fisher Scientific, Inc.) was used to provide calcium ions. Reagent grade HCl and NaOH (Fisher Scientific, Inc.) were used to adjust the pH of all samples. Potassium chloride (>99%, Fisher Scientific, Inc.) was used as the supporting electrolyte. Ultrapure water ($\geq 18.2\ M\Omega \cdot \mathrm{cm}$) was prepared with a Millipore Elix 3-UV followed by a Milli-Q Academic purification system.

3.2.2 Sample Preparation

A background electrolyte of 1 mM KCl was included in all samples, and the pH of all samples was adjusted to 9, which is similar to the pH in tailing slurries in the oil sands industry. The bitumen-in-water emulsion and clay suspensions were prepared using a similar ultrasonic method to Liu et al. (2002) with slight differences. About 0.3 g of bitumen was placed in 30 ml of 1mM KCl at pH 9 and emulsified using a Fisher Scientific Model 500 ultrasonic dismembrator for 20 min using a ½" horn at an amplitude of 70. The clay suspensions were prepared by adding 0.3 g clay to 3 ml of 1 mM KCl and placing in an ultrasonic bath (Fisher Scientific, Inc.) for 15 min. Other ions (CaCl2 and Na3Cit) to be tested were added to the emulsion and suspension prior to sonication. A Mastersizer 3000 (Malvern, UK) laser diffraction particle size analyzer

was used to determine the volume-based passing size (d_{50}) of the bitumen emulsion and montmorillonite, kaolinite clay suspensions in 1 mM KCl at pH 9, with values measured to be 50.8 µm, 7.05 µm and 8.88 µm, respectively.

To prepare a bitumen-clay mixture, 20 g of bitumen emulsion and 10 g of clay suspension were mixed and placed in an ultrasonic bath for around 15 min. For zeta potential distribution measurements, all samples were diluted to a 0.01-0.1 wt% concentration into a solution of the desired test composition. Sodium citrate was added at different times when preparing bitumen-clay mixtures, as exhibited in Fig. 3.2. Fig. 3.2a shows the sodium citrate was added at the same time as calcium to test whether sodium citrate could prevent slime coating, while Fig. 3.2b shows sodium citrate was added after the bitumen emulsion and clay suspension had been sonicated together to test whether sodium citrate could remove slime coating.

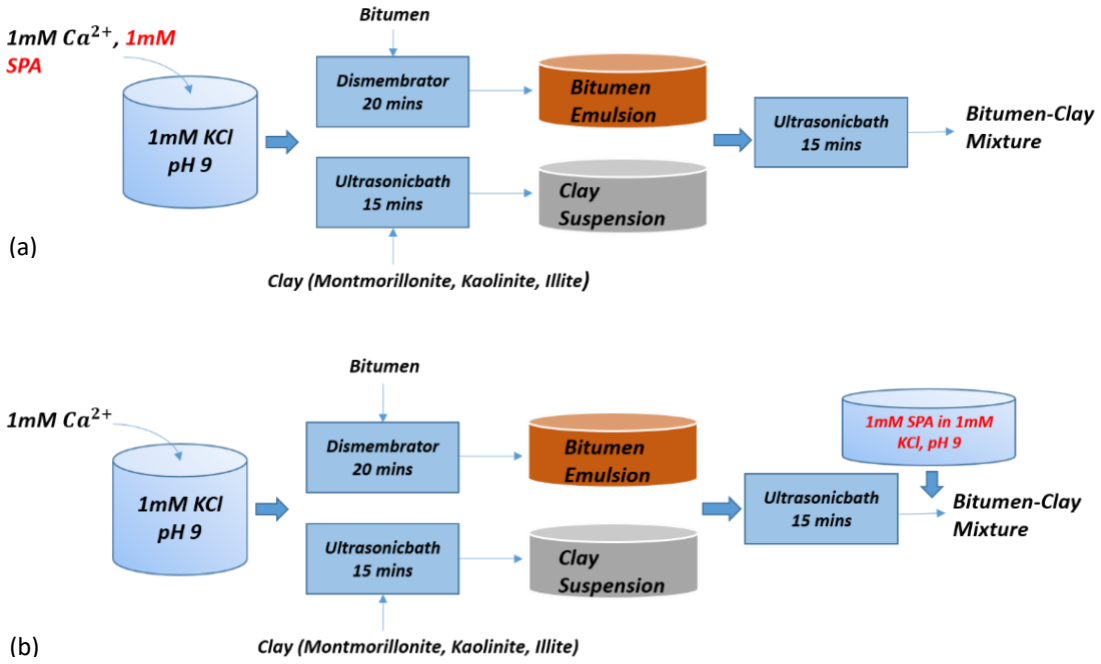

Figure 3.2 Schematic procedures of bitumen-clay mixture preparation. (a) Method 1: the mixture is prepared using the background solution containing both sodium citrate and calcium ions at pH 9; (b) Method 2: the mixture is prepared using the background solution only containing calcium ions and sodium citrate is added after mixing.

3.2.3 Zeta Potential Distribution Measurement Procedure

Zeta potential distributions were measured with a Zetaphoremeter IV (CAD Instruments) by tracking the velocity of 20-100 particles in a known electric field. Upon application of a voltage between two electrodes, the charged particles move toward one or the other electrode within the electrophoresis cell. A laser illuminates the particles, and a CCD camera captures the movement of particles at the stationary layer to reduce electroosmotic effects and accurately determine electrophoretic mobility. Approximately 20 ml of the prepared sample was pulled into the electrophoresis cell via a syringe, and 5 traces of each sample were recorded.

Electrophoretic mobility of each traced particle was determined from the captured video using the built-in software, and electrophoretic mobility distributions were converted to zeta potential distributions using the Smoluchowski equation. The ambient temperature during experiments was maintained at 20 $\pm$ 0.3 ℃.

3.3 Results and Discussion

3.3.1 Individual Bitumen Emulsions and Clay Suspensions

The zeta potential distributions of individual bitumen emulsions and montmorillonite clay suspensions in 1 mM KCl at pH 9 are exhibited in Fig. 3.3a. Both bitumen droplets and montmorillonite clay particles showed negative distributions centred at -75 mV and -22 mV, respectively. With the addition of 1 mM calcium, the magnitude of zeta potentials of both the bitumen emulsion and montmorillonite clay suspension decreased significantly, with distributions centred at -38 mV and -15 mV, respectively (Fig. 3.3b). The significant reduction of zeta potential with the addition of calcium could result from the combination of the following factors: the compression of the electrical double layer, specific adsorption of calcium ions on the bitumen and clay, and the cation exchange of calcium ions for sodium or potassium ions on the clay basal planes. It has been hypothesized that calcium could act as a linker between the bitumen and montmorillonite surface, further enhancing heterocoagulation (Liu et al., 2002). Similar trends were observed by other researchers (Long et al., 2006). Fig. 3.3c shows the zeta-potential distributions of bitumen droplets and montmorillonite particles in the presence of 1 mM sodium citrate and 1 mM KCl at pH 9. Compared to

the zeta potentials of bitumen emulsion and montmorillonite clay suspension in 1 mM KCl (Fig. 3.3a), the addition of 1 mM sodium citrate resulted in more negative zeta potentials with the distributions centred at -85 mV and -40 mV, respectively. The more negative zeta potential distributions of bitumen and montmorillonite clay indicate that, in the presence of citrate, the attachment of clay particles on bitumen is less favourable due to more EDL repulsion. When 1 mM calcium ions and 1 mM sodium citrate were added at the same time in 1mM KCl at pH 9, both bitumen droplets and montmorillonite clay particles displayed a new zeta-potential distribution, with peaks centred at -65 mV and -29 mV respectively. By comparing the results of Fig. 3.3d with Fig. 3.3a and Fig. 3.3b, it was observed that the zeta-potential of bitumen was between that in 1 mM KCl and that in a solution of 1 mM KCl and 1 mM $CaCl_2$, indicating that citrate diminished the impact of calcium ions. However, the zeta-potential of montmorillonite in a solution of 1 mM KCl, 1 mM $CaCl_2$, and 1 mM sodium citrate was slightly more negative than in only 1 mM KCl, suggesting citrate had more influence on the surface charge properties of montmorillonite clay particles. From the electrostatic interaction point of view, citrate could hinder the reduction of the electrical double layer repulsion between bitumen and montmorillonite particles caused by the presence of calcium ions, resulting in less slime coating.

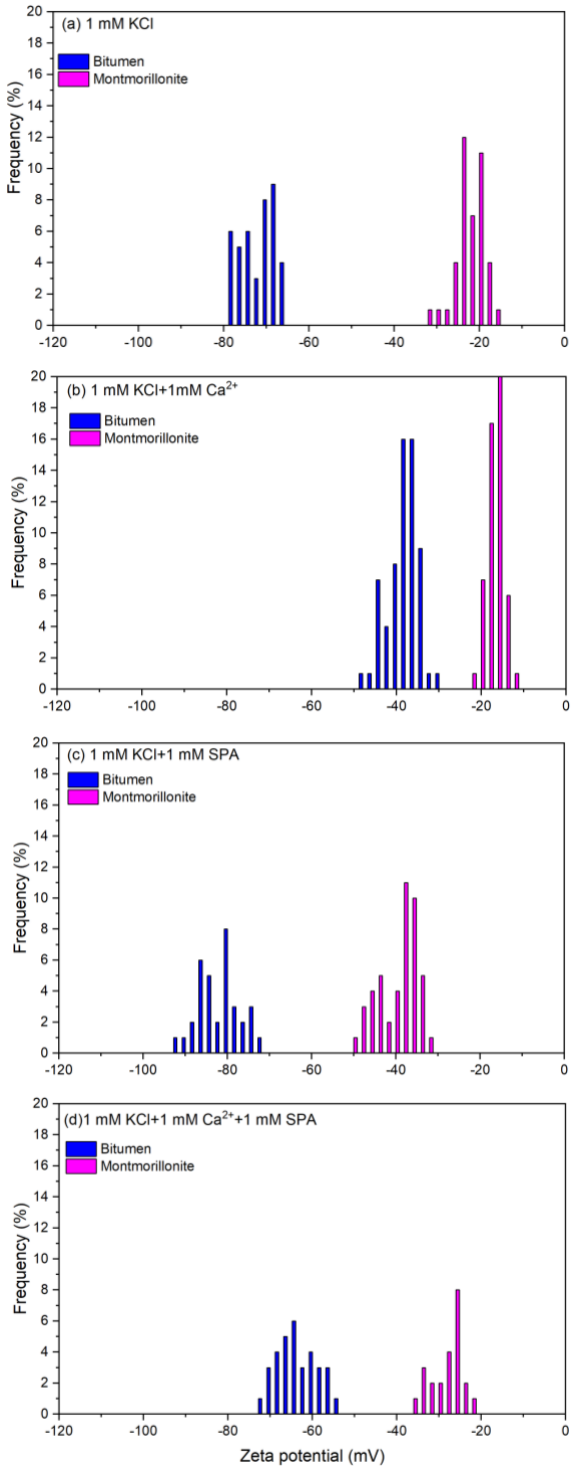

Figure 3.3 Zeta potential distributions for individual bitumen emulsion and montmorillonite clay suspension at pH 9. (a) in 1 mM KCl solution; (b) in 1 mM KCl solution containing 1 mM $CaCl_2$; (c) in 1 mM KCl solution containing 1 mM Na_3Cit; (d) in 1 mM KCl solution in presence of both 1 mM $CaCl_2$ and 1 mM Na_3Cit.

Similar zeta-potential distribution changes were found for kaolinite clay suspensions. In 1 mM KCl solution at pH 9, the zeta-potential distribution of the kaolinite clay suspension was centred at -53 mV, as shown in Fig. 3.4a. While in the presence of 1 mM $CaCl_2$, the zeta-potential distribution peak position shifted to -22 mV, as exhibited in Fig. 3.4b. Fig. 3.4c shows the peak position of kaolinite suspension prepared with the addition of 1 mM sodium citrate in 1 mM KCl of pH 9, from which it was noted that citrate also caused more negative zeta potentials on kaolinite particles as it did for bitumen and montmorillonite. In 1 mM KCl at pH 9 containing both 1 mM sodium citrate and 1 mM $CaCl_2$, the distribution peak shifted back to a position that was slightly more positive than the one measured in 1 mM KCl solution alone, as shown in Fig. 3.4d. Based on the results above, the same conclusion could be drawn that citrate can weaken the impact of calcium on changing surface charge properties of both bitumen droplets and kaolinite particles. From these individual distributions, it appears that sodium citrate effectively chelates with calcium ions or otherwise reduces the influence of calcium on the surfaces of bitumen, montmorillonite, and kaolinite, which may prevent calcium ions from working as a linker between bitumen droplets and clay particles. However, the proximity of the bitumen and kaolinite distributions indicate that drawing conclusions from zeta potential measurements may be difficult for the mixed bitumen-kaolinite system.

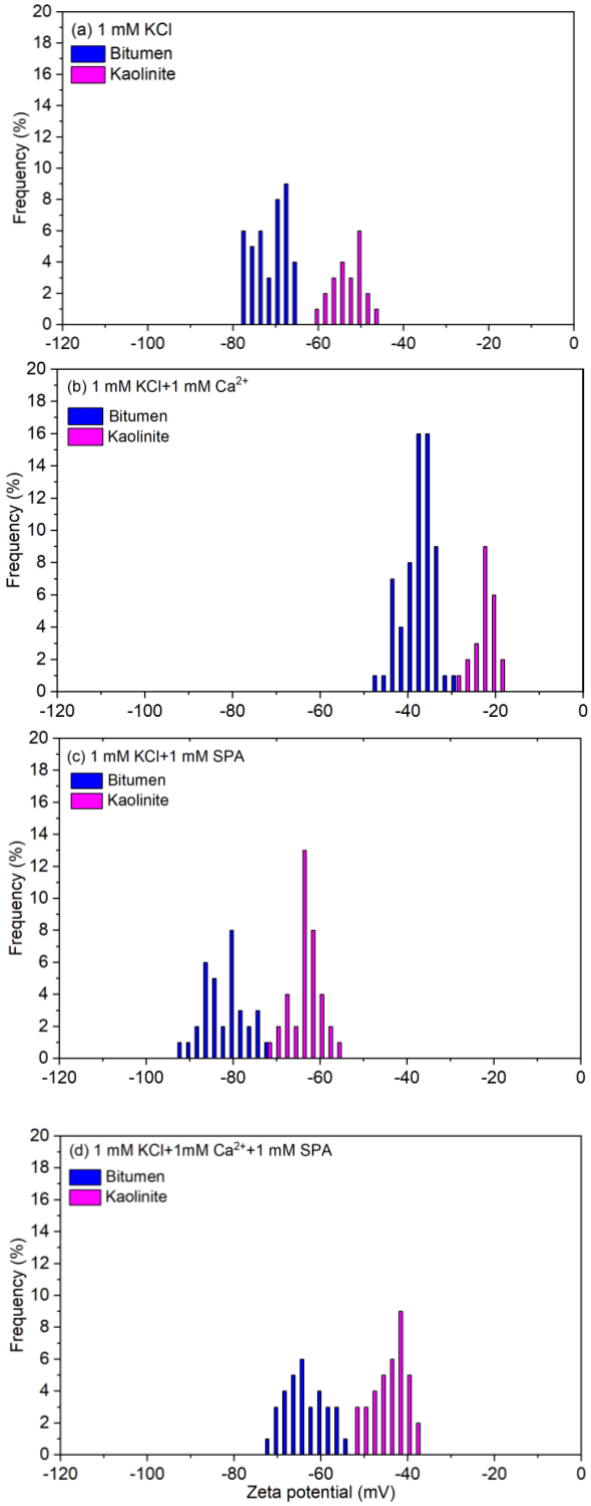

Figure 3.4 Zeta potential distributions for individual bitumen emulsion and kaolinite clay suspension at pH 9. (a) in 1 mM KCl solution; (b) in 1 mM KCl solution containing 1 mM $CaCl_2$; (c) in 1 mM KCl solution containing 1 mM Na_3Cit; (d) in 1 mM KCl solution in presence of both 1 mM $CaCl_2$ and 1 mM Na_3Cit.

3.3.2 Bitumen-Montmorillonite Mixture

The zeta-potential distribution of a bitumen-montmorillonite mixture at a mass ratio of 1:0.5 (bitumen emulsion:clay suspension) measured in 1 mM KCl solution is shown in Fig. 3.5b. The distribution is much broader with a centre position around -40 mV, falling between the zeta potential peaks of individual bitumen droplets and montmorillonite clay particles. In this condition, the bitumen droplets were just partially covered by montmorillonite particles with some amount of unattached montmorillonite clay particles remaining in suspension. With the addition of 1 mM calcium, a strong unimodal distribution was observed at the location corresponding to that of the individual montmorillonite clay suspension (Fig. 3.3c). This single peak indicates calcium ions enhanced the coverage of montmorillonite clay particles on the bitumen droplets, causing complete coverage of the bitumen droplet surfaces by montmorillonite particles. In the case when 1 mM sodium citrate was added at the same time with 1 mM calcium in 1 mM KCl solution at pH 9, as described in Fig. 3.2a, two separate zeta potential peaks were observed at -58 mV and -29 mV, respectively, which are similar to those measured for individual bitumen emulsion and montmorillonite suspension in the same solution. It can be concluded that there was no coagulation between bitumen droplets and montmorillonite clay particles and all the montmorillonite particles were still left in the suspension. This result shows that when added prior to the interaction between bitumen and montmorillonite, sodium citrate can diminish the impact of calcium ions on promoting slime coating and prevent slime coating from occurring.

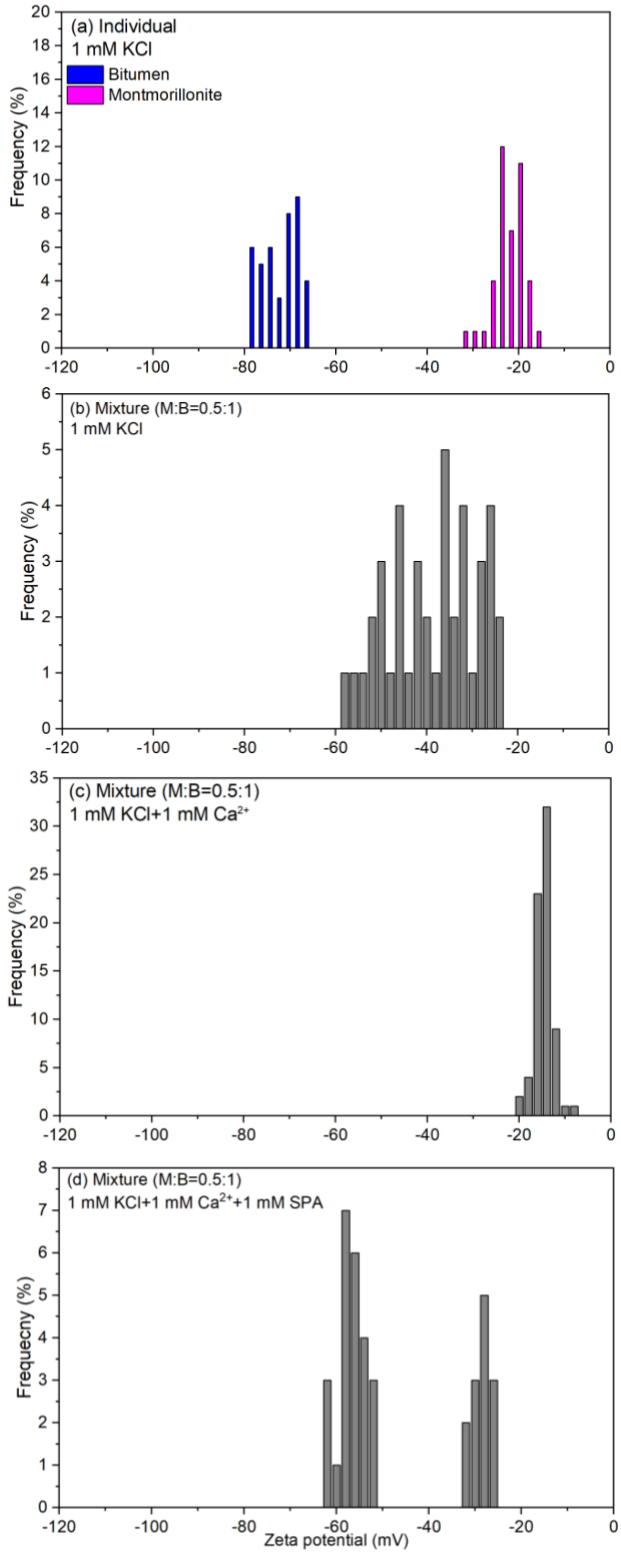

Figure 3.5 Zeta potential distributions in 1 mM at pH 9 for (a) individual bitumen emulsion and montmorillonite clay suspensions, (b) their mixture, (c) their mixture with 1 mM $CaCl_2$, (d) their mixture in 1 mM $CaCl_2$ and 1 mM Na_3Cit.

To test whether citrate could remove a slime coating that had already formed, citrate was added after the bitumen-montmorillonite mixture had been prepared in the presence of calcium, as illustrated in Fig. 3.2b. The zeta potential distribution of the mixture was measured, and a single peak was found at a magnitude between that of individual bitumen and montmorillonite (Fig. 3.6c). The presence of a single peak indicated citrate could only make the montmorillonite particles attached on the surfaces of bitumen droplets more negatively charged and could not make the clay particles detach from bitumen droplets. Thus, citrate could not remove slime coating once it had already occurred.

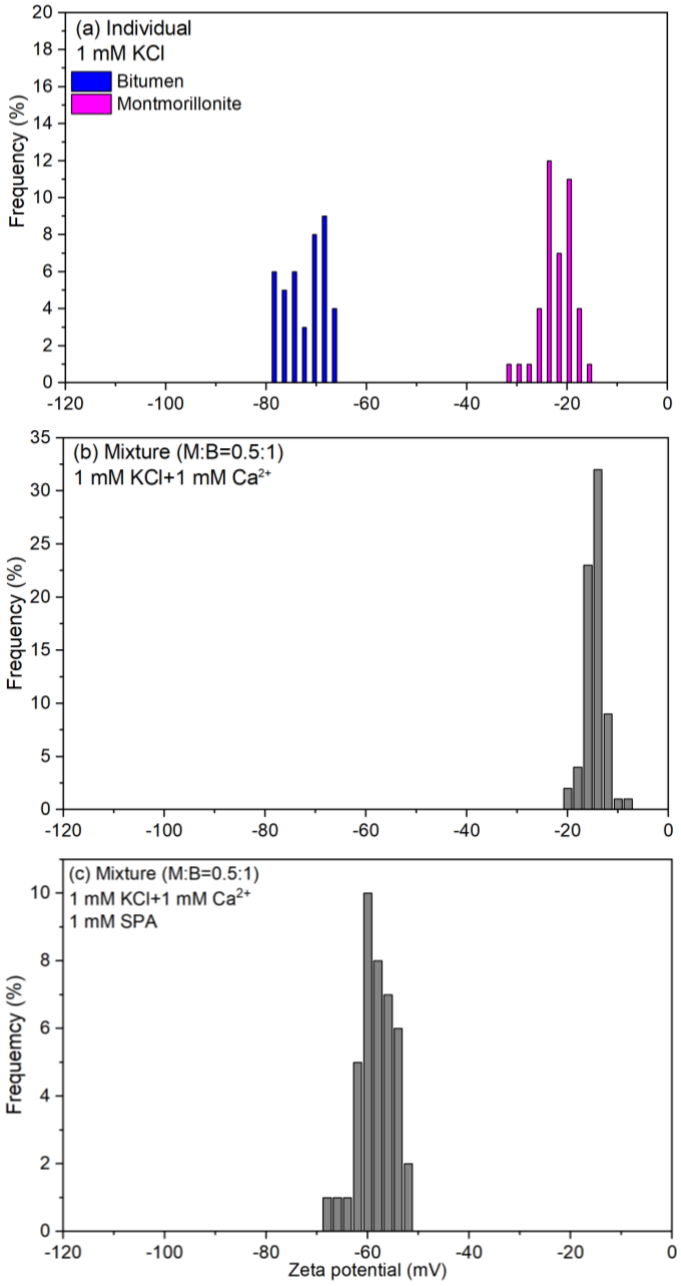

Figure 3.6 Zeta potential distributions in 1 mM KCl at pH 9 for (a) individual bitumen emulsion and montmorillonite clay suspension, (b) their mixture with 1 mM $CaCl_2$, (c) their mixture with 1 mM $CaCl_2$ and later addition of 1 mM Na_3Cit.

3.3.3 Role of Sodium Citrate Dosage in Slime Coating

Since zeta potential distribution analysis showed citrate was able to prevent slime coating of montmorillonite onto bitumen droplets, a subsequent experiment was conducted to determine the effect of citrate dosage on preventing slime coating. Bitumen-montmorillonite mixtures were prepared in 1 mM KCl + 1 mM $CaCl_2$ at pH 9, and a sodium citrate dosage range of 0.5 mM to 1 mM was added before mixing, as described in Fig. 3.2a. From the zeta potential distributions of the bitumen-montmorillonite mixtures (Fig. 3.7), it can be noted that the addition of citrate caused the distributions to shift to more negative zeta potentials and the difference between the two distributions became larger with higher citrate concentrations. These trends suggest that higher concentrations of citrate better prevent slime coating of montmorillonite on bitumen droplets, which could be explained by the complexation reaction between calcium ions and citrate at pH 8.5: $\mathrm{Ca^{2+} + Cit^{3-} \rightleftharpoons CaCit^{-}}$, as shown in previous research (Gan et al., 2009).

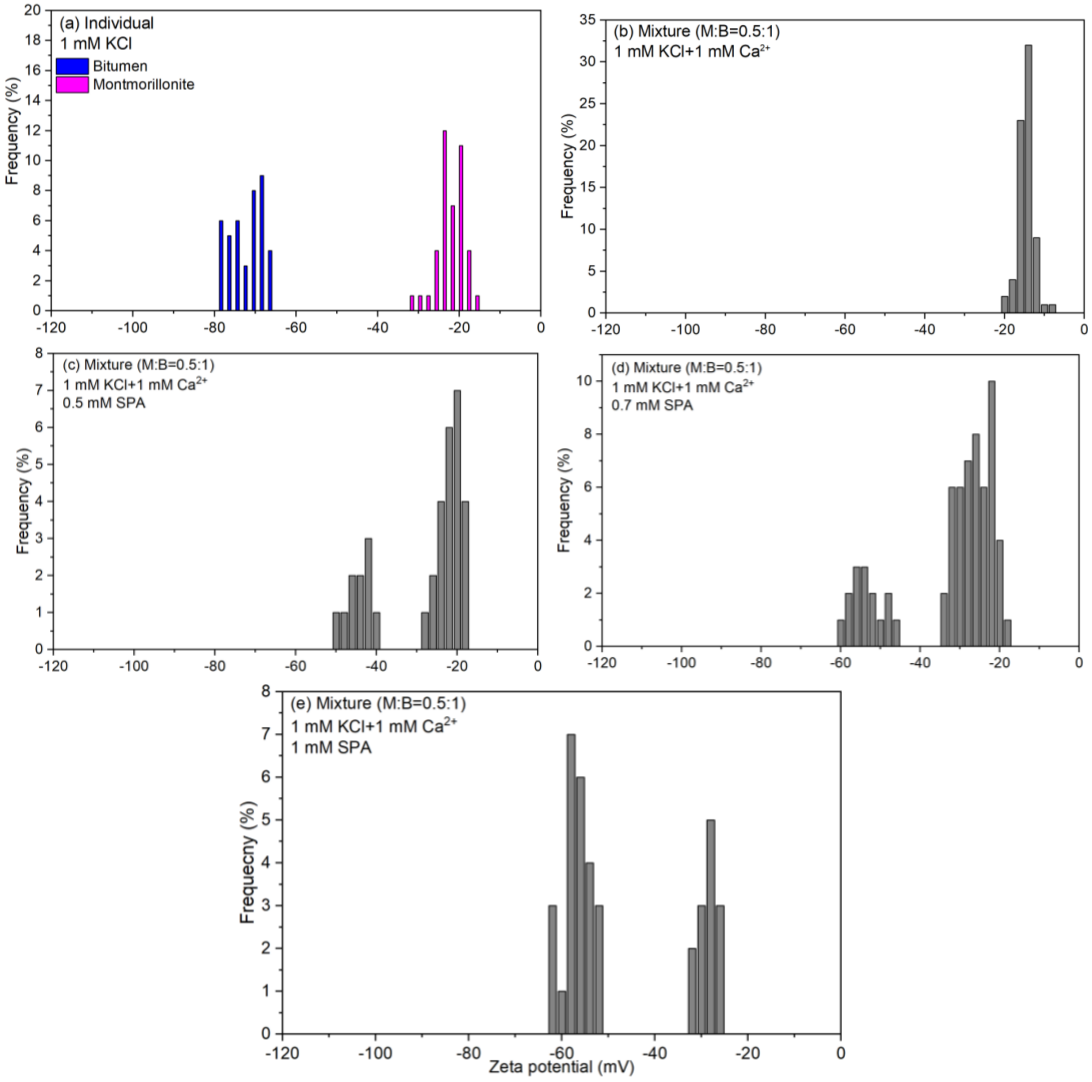

Figure 3.7 Zeta potential distributions in 1 mM KCl at pH 9 for (a) individual bitumen emulsion and montmorillonite clay suspension, (b) their mixture with 1 mM $CaCl_2$, (c), their mixture with 1 mM $CaCl_2$ and 0.5 mM Na_3Cit, (c) their mixture with 1 mM $CaCl_2$ and 0.7 mM Na_3Cit, (e) their mixture with 1 mM $CaCl_2$ and 1 mM Na_3Cit.

3.3.4 Bitumen-Kaolinite Clay Mixture

The zeta potential distribution of bitumen-kaolinite mixture at a 1:0.5 mass ratio (bitumen emulsion:clay suspension) in 1 mM KCl at pH 9 is shown in Fig. 3.8b. A broad, multimodal distribution was observed, indicating a weak attraction between these two components and a substantial amount of unattached bitumen droplets and kaolinite particles. With the addition of 1 mM $CaCl_2$, a distribution with a broader range than that of the bitumen-montmorillonite mixture was observed, shown in Fig. 3.8c, which suggests only partial coverage of bitumen droplets by kaolinite or no coating at all. When the bitumen emulsion and kaolinite clay suspension were prepared with the addition of both 1 mM $CaCl_2$ and 1 mM sodium citrate in 1 mM KCl solution at pH 9 and mixed at a mass ratio of 1:0.5 as described in Fig. 3.2a, the zeta potential distribution of the mixture had two distinguishable peaks centred at -68 mV and -45 mV, respectively, corresponding to those measured for bitumen emulsion and kaolinite suspension individually. Although the findings for kaolinite are less conclusive than those for montmorillonite, it appears kaolinite exhibited less propensity for slime coating than montmorillonite under the tested conditions, and, like for montmorillonite, sodium citrate was able to reduce the severity of slime coating of kaolinite on bitumen when calcium was present.

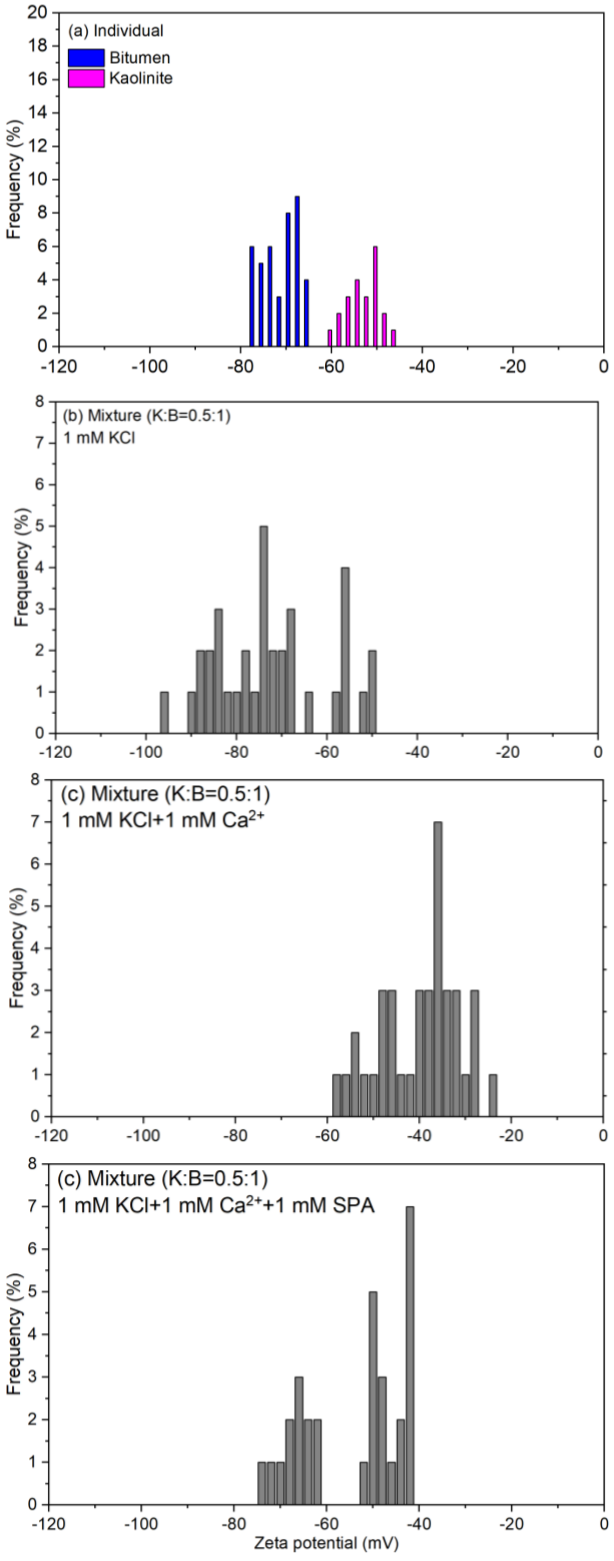

Figure 3.8 Zeta potential distributions in 1 mM KCl at pH 9 for (a) individual bitumen emulsion and kaolinite clay suspension, (b) their mixture, (c) their mixture with 1 mM $CaCl_2$, (d) their mixture with 1 mM $CaCl_2$ and 1 mM Na_3Cit.

To test whether sodium citrate could remove kaolinite slime coatings from bitumen, the bitumen-kaolinite mixture was prepared as described in Fig. 3.2b. A bimodal zeta potential distribution with peaks centred at -69 mV and -62 mV was found (Fig. 3.9c). The peak centred at -62 mV corresponds well to kaolinite in citrate solution (Fig. 3.4c), whereas the peak centred at -69 mV is similar in magnitude to that of bitumen in a solution containing both calcium and citrate (Fig. 3.4d). One explanation for this behaviour is that calcium preferentially adsorbs onto or binds with bitumen, leaving a lower concentration of Ca^{2+} in solution to adsorb onto kaolinite. When citrate is then added, the citrate can remove the adsorbed Ca^{2+} from kaolinite surface, shifting the zeta potential more negative. The citrate can also interact with the Ca^{2+} on the surface of the bitumen remove all of it, causing an intermediate zeta-potential between that in calcium solution and that of citrate solution. Thus, the bimodal zeta-potential distribution in Fig. 3.9c either suggests the kaolinite did not form a slime coating on bitumen in the presence of calcium or that citrate was able to remove the kaolinite slime coating. In either scenario, kaolinite had a much lower propensity for forming a slime coating than montmorillonite, and citrate reduced the ability even more.

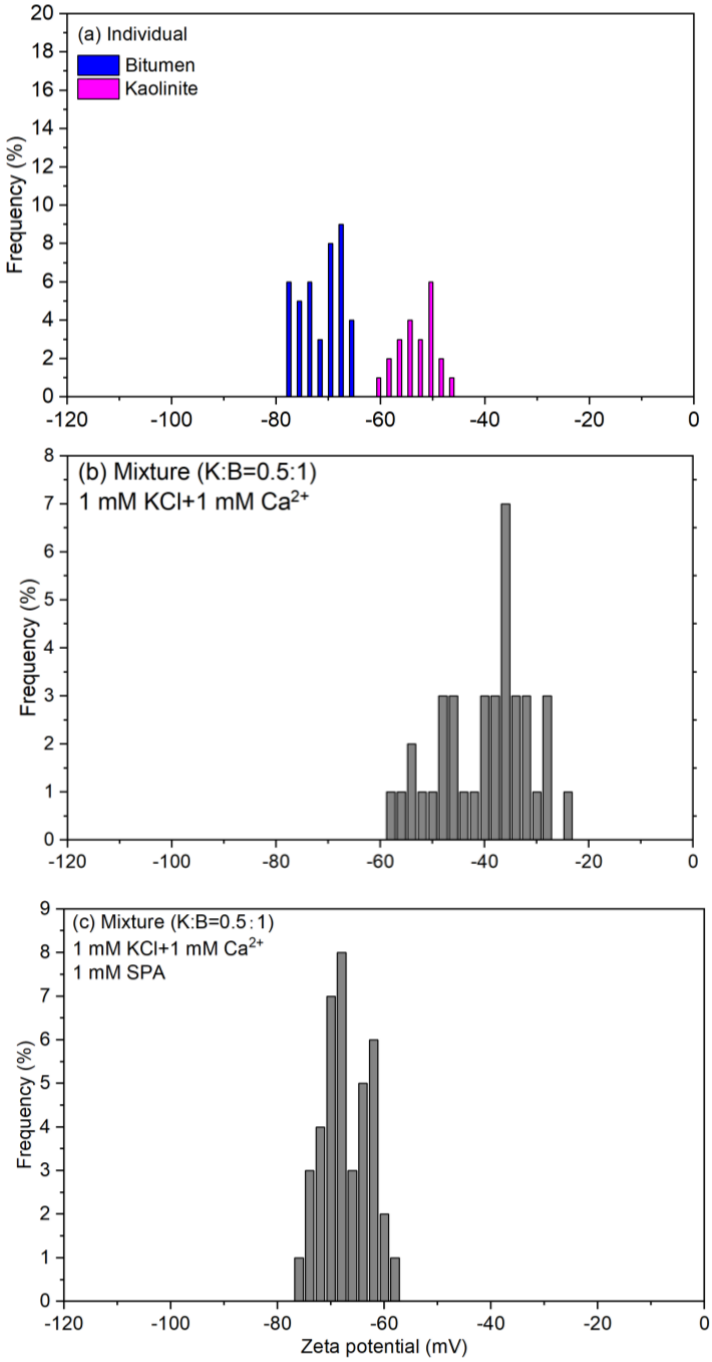

Figure 3.9 Zeta potential distributions in 1 mM KCl at pH 9 for (a) individual bitumen emulsion and kaolinite clay suspension, (b) their mixture in 1 mM $CaCl_2$, (c) their mixture in 1 mM $CaCl_2$ with the addition of 1 mM Na_3Cit later.

CHAPTER 4

4 QCM-D Measurement

Quartz crystal microbalance with dissipation monitoring (QCM-D) has been widely used as a powerful tool to characterize and quantify the interactions between bitumen and different types of clays causing slime coating in the oil sands industry (Bakhtiari et al., 2015). In this study, the QCM-D technique was chosen to investigate the effect of sodium citrate on preventing and breaking bitumen-clay coagulation and to verify the conclusions based on zeta potential distribution results.

4.1 Principles of the Technique

The core part of QCM-D is the quartz piezoelectric sensor with conducting metal films on each side of it. The quartz crystal sensor oscillates under an applied alternating voltage to the metal films, and the oscillation frequency is related to the mass of the sensor. Therefore, a common application of QCM-D is to qualitatively and quantitatively determine the deposition of molecules and particles on the piezoelectric sensor by monitoring the frequency change, Δf. The relationship between the deposited area-normalized mass ($\Delta m, \mathrm{ng/cm^2}$) on the sensor and its related resonant frequency shift was first formalized by (Sauerbrey, 1959), as shown in Eq. 4.1 and Eq. 4.2 (Chen et al., 2016).

$$-\Delta \mathrm{f} = \frac{n f_0 \Delta m}{\rho_q t_q} = \frac{n \Delta m}{c} \tag{4.1}$$

$$\Delta m = -\frac{C\Delta f}{n} \tag{4.2}$$

Where n is the overtone number, f_0 is the fundamental resonance frequency, ρ_q is the density of the quartz crystal, t_q is the thickness of the quartz crystal, and c is the sensitivity constant (17.7 $\mathrm{ng \cdot cm^{-2} \cdot Hz^{-1}}$ for a 5 MHz quartz resonator).

According to the Sauerbrey equation, a negative frequency shift indicates an apparent mass increase of the sensor and suggests the deposition of clay particles on the sensor. However, the Sauerbrey equation was developed for a rigid layer of materials deposited in air or vacuum, and most systems studied do not satisfy this condition. For such systems, the deposited film may exhibit viscoelastic properties. The frequency would be influenced by the mechanical properties of the deposited film, including the shear modules and viscosity (Cho et al., 2007). Thus, it is more appropriate to use both frequency and dissipation responses to describe the apparent mass increase on the sensor surface. When the sensor dissipation shift is considered to be > 5% of frequency shift, the mass of the deposited viscoelastic film can be modelled using the Voinova – Voigt equation (Bakhtiari et al., 2015). The changes of frequency (Δf) and dissipation (ΔD) caused by the presence of the viscoelastic film is defined as below (Voinova et al., 1999).

$$\Delta f \approx -\frac{1}{2\pi\rho_0 h_0}\left\{\frac{\eta_2}{\delta_2} + h_1\rho_1\omega - 2h_1\left(\frac{\eta_2}{\delta_2}\right)^2 \frac{\eta_1\omega^2}{{\mu_1}^2 + \omega^2{\eta_1}^2}\right\} \tag{4.3}$$

$$\Delta D \approx \frac{1}{2\pi f\rho_0 h_0}\left\{\frac{\eta_2}{\delta_2} + 2h_1\left(\frac{{\eta_2}^2}{\delta_2}\right)\frac{\eta_1\omega^2}{{\mu_1}^2 + \omega^2{\eta_1}^2}\right\} \tag{4.4}$$

$$\delta_2 = \sqrt{\frac{2\eta_2}{\rho_2 \omega}} \tag{4.5}$$

Where subscripts 0, 1, and 2 refer to the quartz, deposited viscoelastic film, and bulk fluid, respectively, and h is thickness, ρ is density, η is viscosity, μ is shear modulus, and ω is the angular frequency of oscillation.

4.2 Materials and Methods

4.2.1 Materials

Vacuum distillation unit (VDU) feed bitumen was provided by Syncrude Ltd., Canada. Silica sensors (QSX 303, Biolin Scientific) were purchased from Nanoscience Instruments. Montmorillonite and kaolinite clay were obtained from Ward's Minerals. Reagent-grade toluene (Fisher Scientific, Inc.) was used as a cleaning solvent and to prepare a 5 wt% toluene-diluted bitumen solution. All other chemicals used were the same as the ones described for zeta potential distribution measurement.

4.2.2 QCM-D Sensor Preparation

For QCM-D measurement, the procedures given in (Bakhtiari et al., 2015) to prepare the bitumen-coated piezoelectric quartz sensors were followed with some changes to the spin coating portion. New silica sensors were first treated with UV/ozone for 10 min, rinsed with Milli-Q water, and dried with nitrogen gas to ensure a hydrophilic surface. This was repeated twice before hydrophobic treatment. The hydrophilic sensors were then exposed to dichlorodimethylsilane (DDMS, Fisher Scientific) vapour

for 5 min, rinsed with Milli-Q water, and dried with nitrogen gas. The contact angle of the sensors after hydrophobic treatment was determined to be 85°, as shown in Fig. 4.1b. In this study, a spin coater (Laurell WS-400A-6NPP/Lite) was used to coat a thin bitumen film on the hydrophobically-treated silica sensors. To obtain a smooth bitumen film, 5 drops of the toluene-diluted bitumen were added dropwise to the sensor while it rotated at 2500 rpm for 40. Then the sensor was rotated at 4500 rpm for another 50 s to remove excess toluene and form a uniform surface.

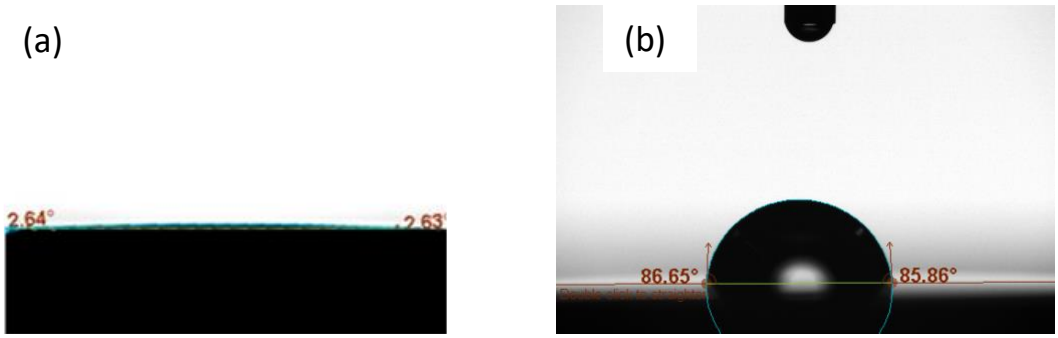

Figure 4.1 Contact angle of (a) piezoelectric quartz sensor, (b) hydrophobized piezoelectric quartz sensor.

4.2.3 Sample Preparation

Clay suspensions were prepared by adding 0.1 wt% clay to 1 mM KCl at pH 8.5 with or without the addition of other chemicals. The suspensions were then sonicated with a Fisher Scientific Model 500 ultrasonic dismembrator for 30 min. The volume-based passing sizes (d_{50}) of montmorillonite and kaolinite after sonication were measured to be 3.48 μm and 3.64 μm, respectively, using a Mastersizer 3000 (Malvern, UK). The pH for all samples was adjusted to 8.5 after preparation since preliminary studies

showed more liberation of the bitumen from the coated sensor at pH values greater than about 9.

4.2.4 QCM-D Measurement Procedure

The frequency and dissipation shifts of the bitumen-coated sensor were monitored by a Q-Sense E4 (Biolin Scientific). Prior to each experiment, the flow module, connecting tubes were washed thoroughly by sonicating in a 2% SDS solution with copious rinsing in Milli-Q water to avoid the impact of any organic contaminations on results. The E4 unit was inverted to avoid clay particle deposition from gravity and ensure any deposition was a consequence of colloidal forces. All experiments were conducted at 22 ± 0.02 ℃ and repeated twice. The flow rate was maintained at 0.12 $\mathrm{mL/min}$. The frequency and dissipation shifts of the third overtone were used for calculations and analysis using the Q-Tools software. To better examine the effectiveness of sodium citrate, the calcium concentration in samples was adjusted to 5 mM to obtain strong bitumen-clay coagulation.

4.3 Results and Discussion

4.3.1 Montmorillonite

To further confirm the effect of sodium citrate on slime coating investigated by zeta potential distribution measurement, the interactions between bitumen and montmorillonite clay particles in the absence and presence of sodium citrate was studied by QCM-D technique. The technique was first validated by measuring the

interaction between bitumen and montmorillonite in 1 mM KCl with or without the addition of calcium. For all the experiments, baseline frequency and dissipation shifts were established using the desired solutions without added clay. Fig. 4.2 shows the frequency and dissipation responses of the bitumen-coated sensor in 1 mM KCl without the addition of calcium, from which it can be observed that both the frequency and dissipation responses remained largely unchanged when clay was introduced, indicating no deposition of montmorillonite clay particles on the sensor surface.

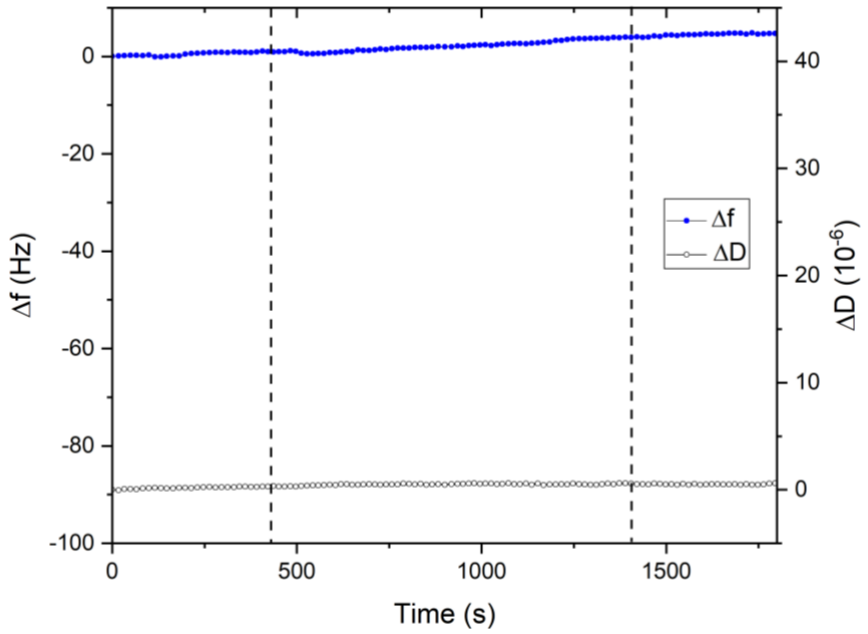

Figure 4.2 Frequency and dissipation responses of bitumen-coated sensor in 1 mM KCl solution at pH 8.5 (background solution). Dashed lines indicate fluid switch (from left to right: background solution to 0.1 wt% montmorillonite clay suspension; Milli-Q water risen).

The frequency and dissipation shifts of the third overtone due to the interaction between bitumen and montmorillonite in a solution containing 5 mM $CaCl_2$ are shown

in Fig. 4.3. Prior to pumping clay suspension into the flow module, a solution of 5 mM $CaCl_2$ and 1 mM KCl at pH 8.5 was introduced into the system to determine the frequency shift that might be due to the interaction of calcium with bitumen. After the montmorillonite clay suspension had been introduced into the flow cell long enough for the frequency shift to stabilize, Milli-Q water at pH 8.5 was used to wash the sensor surface to guarantee the montmorillonite clay particles were strongly attached to the sensor and could not be removed. Comparing Fig. 4.2 and Fig. 4.3, it is clear that in the presence of calcium, the frequency response of the sensor reduced nearly 60 Hz (Fig. 4.3). A negative frequency shift indicates a gain of mass according to the Sauerbrey equation, suggesting that calcium could promote the slime coating of montmorillonite. The apparent mass of montmorillonite particles deposited on the bitumen-coated sensor was calculated by fitting experimental data to the Voigt model with the Q-Tools software to be 1 $\mu g/cm^2$, as shown in Fig. 4.4.

Images of the bitumen-coated sensor were collected using an optical microscope (Fig. 4.5) and scanning electron microscope (SEM) (Fig 4.6) before and after the QCM-D experiments to verify the particle deposition. Comparing images taken before and after experiments, it is obvious that a layer of particles had deposited on the sensor surface.

To test whether SPA could remove montmorillonite slime coating from bitumen, 5 mM SPA and 1 mM KCl at pH 8.5 was introduced into the flow module for 10 min after apparent deposition of montmorillonite particles on the sensor, as seen at

approximately 5500 s in Fig. 4.3. The frequency decreased dramatically, while the dissipation increased, indicating sodium citrate deposited on the bitumen-coated sensor rather than removing montmorillonite clay particles from the sensor. It could also be noticed from Fig. 4.4 that the mass deposition increased by approximately 0.4 $\mu g/cm^2$ with the addition of 5 mM sodium citrate, suggesting that sodium citrate also deposited on the sensor surface covered by montmorillonite particles. Hence, it can be concluded that sodium citrate cannot remove slime coating if it has already occurred, which is consistent with the zeta potential distribution results.

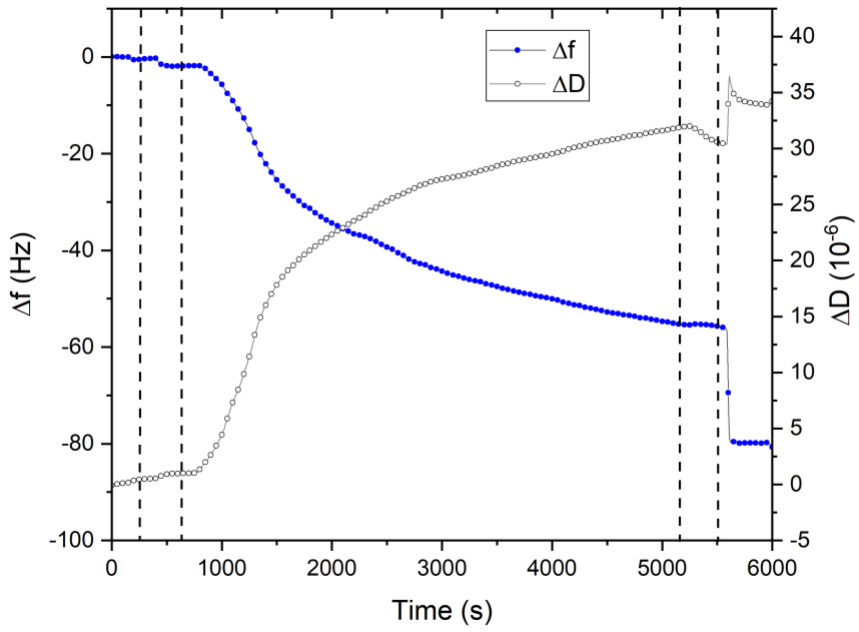

Figure 4.3 Frequency and dissipation responses of a bitumen-coated sensor in 1 mM KCl solution at pH 8.5. Dashed lines suggest fluid switch (from left to right: 1 mM KCl to 1 mM KCl + 5 mM $CaCl_2$; 1 mM KCl + 5 mM $CaCl_2$ to 1 mM KCl + 5 mM $CaCl_2$ + 0.1 wt% montmorillonite clay suspension; Milli-Q water rinse; Milli-Q water to 1 mM KCl + 5 mM Na_3Cit).

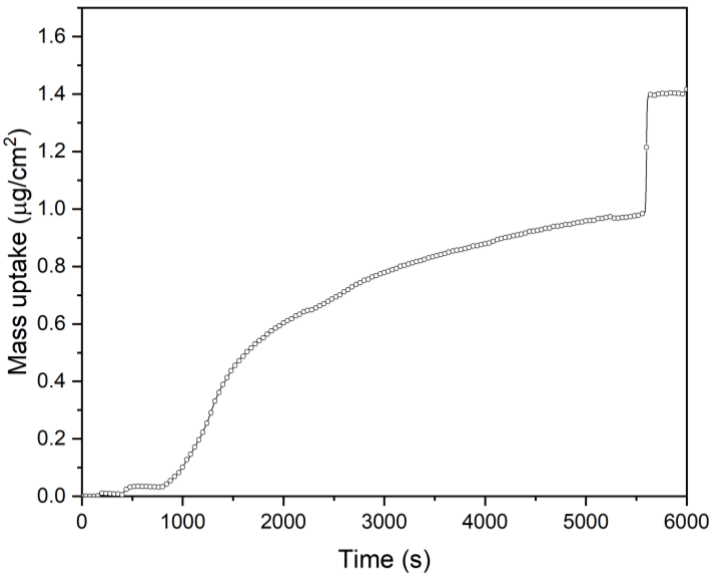

Figure 4.4 Mass uptake of the bitumen-coated sensor for the experimental results shown in Fig. 4.3.

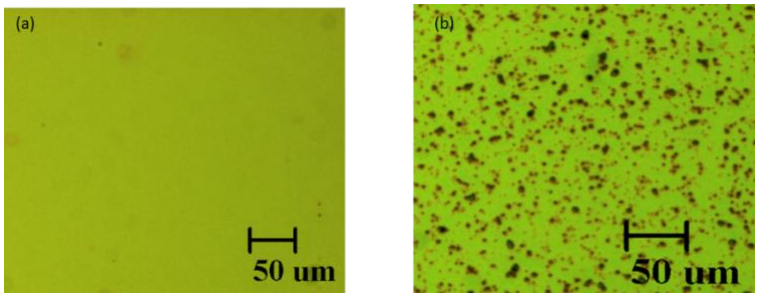

Figure 4.5 Optical microscope images of a bitumen-coated sensor surface taken (a) before and (b) after experiments a QCM-D experiment. Fluid conditions: 0.1 wt% montmorillonite clay suspension in 1 mM KCl + 5 mM $CaCl_2$ at pH 8.5.

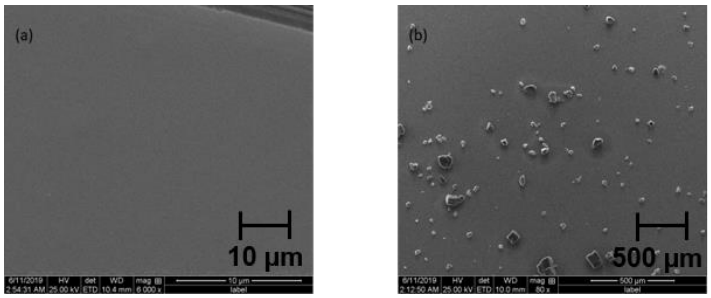

Figure 4.6 SEM images of a bitumen-coated sensor surface taken (a) before and (b) after experiments. Fluid conditions: 0.1 wt% montmorillonite clay suspension in 1 mM KCl + 5 mM $CaCl_2$ at pH 8.5.

To test whether sodium citrate could prevent slime coating of montmorillonite on bitumen, a 0.1 wt% montmorillonite clay suspension was prepared in a solution of 5 mM $CaCl_2$, 5 mM sodium citrate, and 1 mM KCl at pH 8.5. Prior to introducing this suspension to the bitumen-coated sensor, a solution of 5 mM $CaCl_2$, 5 mM sodium citrate, and 1 mM KCl at pH 8.5 was pumped into the flow cell to ensure the frequency and dissipation changes were not caused by any of these ions. As shown in Fig. 4.7, when the montmorillonite clay suspension was introduced, the frequency shift in this experiment was significantly less than without citrate (Fig. 4.3), suggesting reduced deposition of montmorillonite particles on the sensor. Thus, sodium citrate largely prevented slime coating from occurring. This conclusion is consistent with the findings from the zeta potential results as well.

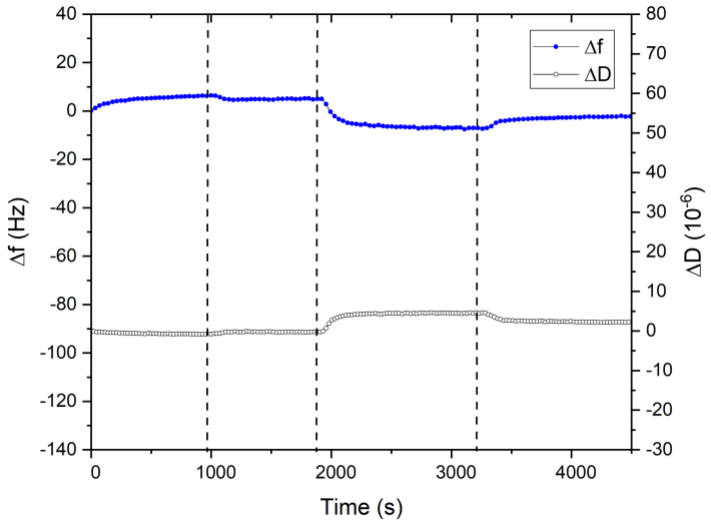

Figure 4.7 Frequency and dissipation responses of a bitumen-coated silica sensor to a montmorillonite clay suspension in the presence of both 5 mM $CaCl_2$ and 5 mM Na_3Cit in 1 mM KCl at pH 8.5. Dashed lines suggest fluid switch (from left to right: 1 mM KCl to 1 mM KCl + 5 mM $CaCl_2$ + 5 mM Na_3Cit; 1 mM KCl + 5 mM $CaCl_2$ + 5 mM Na_3Cit to 0.1 wt% montmorillonite clay suspension + 5 mM $CaCl_2$ + 5 mM Na_3Cit + 1 mM KCl; Milli-Q water rinse).

The adsorption of sodium citrate on bitumen was also studied using QCM-D, as shown in Fig. 4.8. The resonant frequency of the bitumen-coated sensor decreased slightly after the injection of 5 mM sodium citrate at pH 8.5, but the frequency returned to what it was before the injection of citrate when Milli-Q water was introduced into the system. Accordingly, it can be concluded that citrate cannot adsorb on the bitumen surface under this experimental condition. Thus, the substantial frequency drop after the injection of citrate in Fig. 4.3 may result from the adsorption of citrate on montmorillonite clay particles deposited on the bitumen surface.

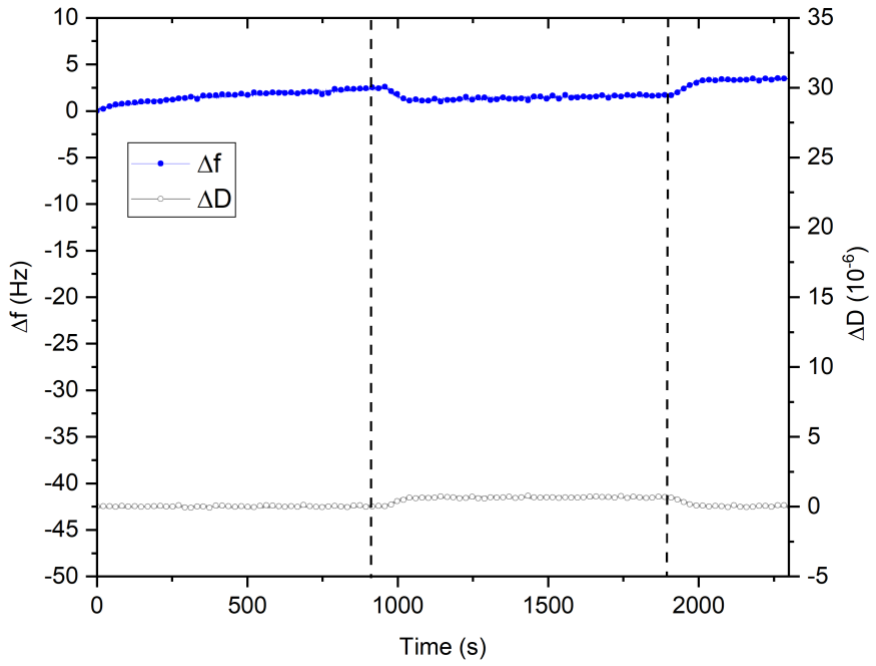

Figure 4.8 Frequency and dissipation responses of the bitumen-coated sensor in 1 mM KCl at pH 8.5 (background solution). Dashed lines suggest fluid switch (from left to right: background solution to 5 mM Na_3Cit in 1 mM KCl; Milli-Q water rinse).

4.3.2 Kaolinite

The interaction between bitumen and kaolinite with the addition of 5 mM calcium was measured with the same procedure as montmorillonite, and the frequency and dissipation responses are shown in Fig. 4.9. It is noted that flowing through 0.1 wt% kaolinite clay suspension in a solution of 5 mM $CaCl_2$ and 1 mM KCl at pH 8.5 only slightly changed the frequency and dissipation responses of the sensor, which suggests that kaolinite caused no slime coating under this condition. This observation is consistent with results from zeta potential distribution measurements. Hence, further experiments to determine the impact of sodium citrate on preventing slime coating caused by kaolinite clay was not conducted.

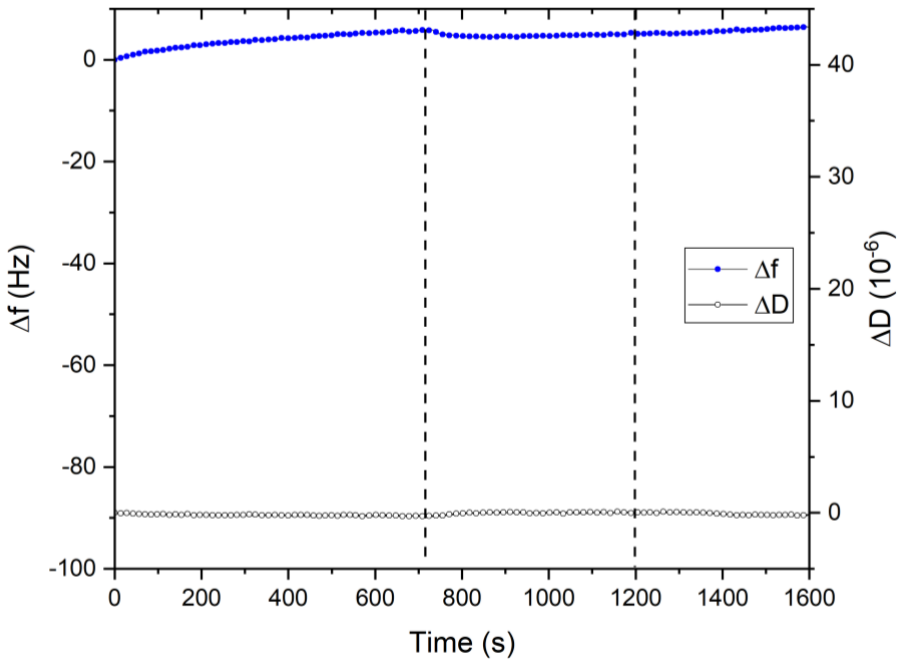

Figure 4.9 Frequency and dissipation responses of the bitumen-coated sensor in 5 mM $CaCl_2$ and 1 mM KCl at pH 8.5 (background solution). Dashed lines suggest fluid switch (from left to right: background solution containing 5 mM $CaCl_2$ to kaolinite clay suspension with the addition of 5 mM $CaCl_2$; Milli-Q water rinse).

CHAPTER 5

5 Calcium Adsorption on Montmorillonite

Adsorption tests were conducted to better understand the role sodium citrate plays in preventing slime coating of montmorillonite clay on bitumen. The impact of sodium citrate on the adsorption of calcium ions on montmorillonite clay particles was studied using batch adsorption tests followed inductively coupled plasma-mass spectrometry (ICP-MS) analysis of the aqueous phase.

5.1 Principles of the Technique

Inductively coupled plasma mass spectrometry (ICP-MS) is widely used for trace multi-element and isotopic analysis. It has numerous advantageous features, including good precision, simple spectra, low detection limits and the ability to analyze isotopes in a short time (Nageswaran et al., 2017). The main components of an inductivity coupled plasma-mass spectroscopy are exhibited in Fig. 5.1.

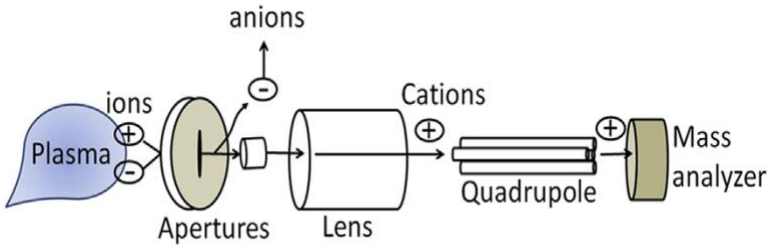

Figure 5.1 The typical configuration of inductivity coupled plasma-mass spectroscopy (ICP-MS) (Singh, 2016). Reprinted with permission from Elsevier.

The principle of ICP-MS is to use an inductively coupled plasma to atomize the introduced sample, dissociate the molecules, remove an electron from the components and form singly-charged ions. Then these ions are directed into a mass filtering device named mass spectrometer. The mass spectrometer separates the ions of interest in the sample based on the mass-to-charge ratios of the ions. Then the ions of interest are detected and amplified to determine their intensities (Abou-Shakra, 2003). Compared to atomic absorption spectroscopy (AAS), ICP-MS features higher precision and sensitivity, and it can analyze several elements simultaneously (Singh, 2016).

5.2 Materials and Sample Preparation

5.2.1 Materials

Montmorillonite clay was purchased from Ward's Minerals. Sodium citrate dihydrate (>99%, Sigma-Aldrich), reagent grade $CaCl_2 \cdot 2H_2O$ (Fisher Scientific, Inc.), and KCl (>99%, Fisher Scientific, Inc.) were used as purchased without further treatment. Reagent grade HCl and NaOH (Fisher Scientific, Inc.) were used to adjust the pH of all samples. Ultrapure water ($\geq 18.2\ M\Omega \cdot \mathrm{cm}$) was prepared with a Millipore Elix 3-UV followed by a Milli-Q Academic purification system.

5.2.2 Sample Preparation

Separate solutions of 40 mM KCl, 40 mM $CaCl_2$, and 40 mM Na_3Cit were prepared in ultrapure water. An approximately 4 wt% montmorillonite clay suspension was

prepared by adding 1.6 g to a vial and bringing the suspension to 40 g with 1 mM KCl. The suspension was shaken vigorously shaken by hand and sonicated for 60 min in an ultrasonic bath (Fisher Scientific, Inc.) to disperse the particles. The suspension was allowed to settle for 48 h and the top 30 ml retained for subsequent use to remove course particles.

For each adsorption test, aliquots of the 40 mM KCl, 40 mM $CaCl_2$, 40 mM Na_3Cit, 4 wt% montmorillonite in 1 mM KCl were added to Milli-Q water to arrive at the desired suspension composition with 0.1 wt% montmorillonite. The pH was then adjusted to 8.45 ± 0.05 using 0.2 M NaOH or 0.2 M HCl. Each suspension was split into 3 separate 30 ml PPCO centrifuge vials that were then shaken at approximately 200 rpm for 60 min on an orbital shaker. The vials were then centrifuged at 5000 RCF for 30 min and the supernatant removed to polypropylene vials for cation determination. The aqueous concentration of calcium was determined by ICP-MS analysis with a Perkin Elmer Elan 6000 instrument. All steps of the batch adsorption experiment were conducted at room temperature (21.0 °C ± 0.5 °C).

One set of samples was prepared to test whether adding citrate after the equilibration of montmorillonite with a calcium solution affected the adsorption differently than adding calcium and citrate together before adding the montmorillonite. For this sample set. A 0.1 wt% montmorillonite suspension was prepared in 1 mM KCl + 1 mM $CaCl_2$, the pH adjusted to 8.45 ± 0.05, and split into 3 vials. The vials were shaken for 30 min at 200 rpm at which point enough 40 mM Na_3Cit was added for a final concentration of 1 mM Na_3Cit. The samples were then shaken for an additional 30

min, centrifuged at 5000 RCF for 30 min and the supernatant retained for ICP-MS analysis.

5.3 Results and Discussion

The calcium concentration released from the montmorillonite clay suspension prepared in different solutions at pH 8.5 was measured, as shown in Fig. 5.1. It was noted that montmorillonite clay released a small amount calcium ions in 1 mM KCl. In the case when montmorillonite clay suspension was prepared in 1 mM KCl with the addition of 1 mM SPA, more calcium ions were released from the montmorillonite clay particles, indicating the addition of SPA promoted the release of calcium ions from montmorillonite clay particles. To ensure the enhanced release of calcium in 1 mM KCl + 1 mM Na_3Cit was not due to cation exchange with the increased concentration of monovalent cation, a sample of montmorillonite clay suspension prepared in 4 mM KCl was also tested. By comparing the aqueous calcium concentration released in 1 mM and 4 mM in Fig. 5.1, it can be concluded that the calcium release was not due to the cation exchange with monovalent cations and citrate was indeed responsible for the enhanced release.

Fig. 5.2 shows the calcium adsorption on montmorillonite clay particles in 1 mM KCl + 1 mM $CaCl_2$ with and without the addition of 1 mM SPA. The adsorbed calcium was calculated by the initial calcium concentration minus the calcium concentration of the supernatant after adsorption. The mass of clay was the same in each sample but was not explicitly measured for normalization. Approximately 0.171 mM $\pm$ 0.014 mM

calcium ions adsorbed on the montmorillonite clay particles in the absence of SPA. When 1 mM calcium chloride and 1 mM sodium citrate were added at the same time, the amount of calcium ions adsorbed on clay particle surfaces decreased to 0.024 mM $\pm$ 0.010 mM. The amount of calcium ions adsorbed on montmorillonite clay particles also decreased when 1 mM sodium citrate was added after prior equilibration of the clay in a solution of calcium chloride. By comparing the results in Fig. 5.2, it can be concluded that sodium citrate can reduce the calcium adsorption on montmorillonite clay particles, no matter when SPA was added.

The results shown in Fig. 5.1 and 5.2 lead to two important findings: (1) citrate can remove calcium ions from clay particle surfaces, and (2) citrate can keep calcium from adsorbing to clay particles. These findings can explain the more negative zeta potential of montmorillonite observed in 1 mM KCl + 1 mM Na_3Cit than that in 1 mM KCl and offer an explanation as to why slime coatings of montmorillonite can be reduced or prevented when citrate is added.

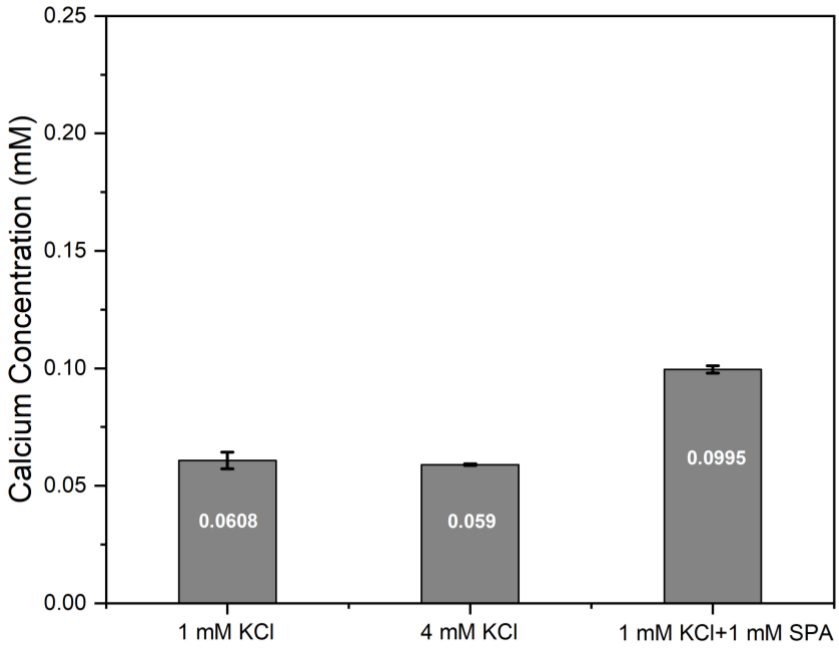

Figure 5.2 Calcium released from montmorillonite clay suspension prepared in different solutions at pH 8.5. From left to right: 1 mM KCl, 4 mM KCl and 1 mM KCl with the addition of 1 mM SPA.

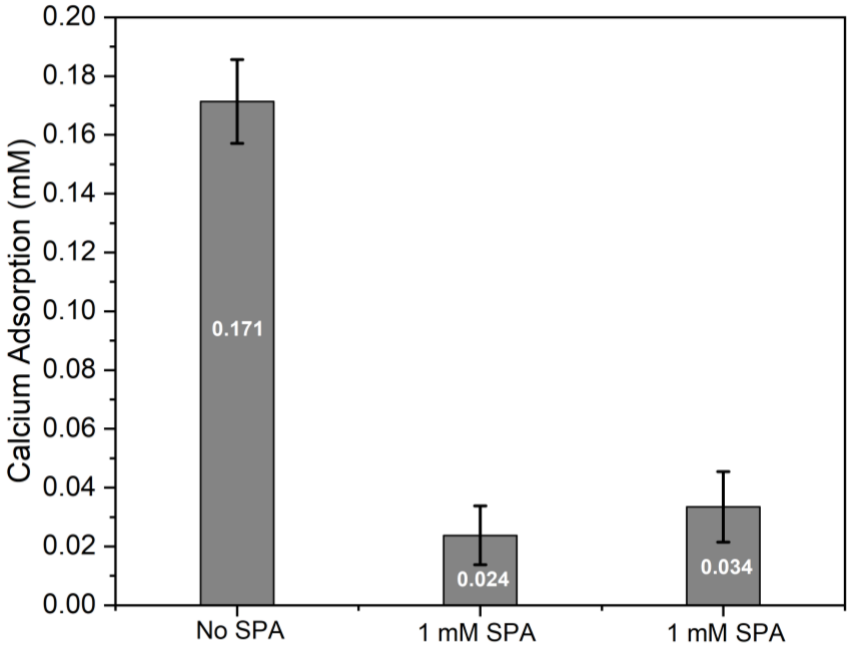

Figure 5.3 Calcium adsorption on montmorillonite clay particles in 1 mM KCl with the addition of 1 mM $CaCl_2$ at pH 8.5. From left to right: no SPA addition; SPA was added at the same time with $CaCl_2$; SPA was added after the addition of $CaCl_2$.

CHAPTER 6

6 Conclusion and Future Work

6.1 Conclusion

In this study, three experimental techniques were used to examine the effect of a secondary processing aid, sodium citrate, on the slime coating of bitumen by clays in the presence of calcium ions. Previously, Liu et al. (2002) found that calcium ions could make the zeta potential values for both bitumen and clays less negative and promote bitumen-clay coagulation, which is detrimental to the bitumen aeration process and can significantly decrease bitumen recovery. Zeta potential distribution measurements in this study were performed to see how sodium citrate affected the zeta potentials of clays and bitumen and whether sodium citrate could prevent slime coatings from occurring.

The addition of sodium citrate made the zeta potential distributions of individual bitumen emulsions and clay suspensions more negative. For both kaolinite and montmorillonite, the zeta potential distribution of the mixture of bitumen and clay stayed nearly unchanged when sodium citrate and calcium chloride were added at the same time, indicating sodium citrate could prevent slime coating from occurring. When a montmorillonite suspension was mixed with a bitumen emulsion in a calcium chloride solution, the zeta potential distribution indicated fully coated bitumen droplets. Adding citrate after formation of this slime coating resulted in a single peak with more negative zeta potential, suggesting that clay particles were not removed.

Thus, citrate could only prevent formation of slime coatings, not remove them. The increased negative surface charge on bitumen and clay surfaces and depressed bridging strength of calcium ions caused by citrate addition were the main reason why citrate could reduce the bitumen-clays attachment and less slime coating.

The increased negative surface charge on bitumen and clay surface and depressed bridging strength of calcium ions caused by citrate addition were the main reason why citrate could reduce the bitumen-clays attachment and less slime coating.

The interactions between bitumen and clays were also measured using QCM-D to further confirm the results from zeta potential distribution measurements. The effect of sodium citrate on preventing bitumen-clay coagulation could still be observed. Without calcium addition, the frequency showed a slight decrease and dissipation showed a slight increase, indicating a weak attraction between montmorillonite clay and bitumen and a marginal slime coating. The frequency decreased significantly and dissipation increased when calcium ions were added with a montmorillonite clay suspension, suggesting a strong attraction between bitumen and montmorillonite clay and hence a severe slime coating. When sodium citrate was then introduced, the frequency continued dropping considerably and the dissipation continued increasing, showing that sodium citrate could not remove slime coating once it had already occurred. When calcium chloride and sodium citrate were added into montmorillonite clay suspension at the same time, the change of frequency and dissipation were marginal, indicating little slime coating. Thus, sodium citrate largely prevented slime coating from occurring. For kaolinite, the change of frequency and dissipation of

bitumen-coated sensor were negligible in the presence of calcium, suggesting weak attraction between kaolinite clay and bitumen and little propensity for formation of slime coating.

To further confirm the results from zeta potential distribution measurement and QCM-D, the adsorption of calcium ions on montmorillonite were studied using batch adsorption experiments and ICP-MS analysis. It was found that sodium citrate could promote the release of calcium ions from montmorillonite clay particles and reduced the adsorption of calcium ions on the montmorillonite clay particles. Both mechanisms help explain why sodium citrate can prevent the slime coating of bitumen by montmorillonite.

6.2 Future Work

1. In the bitumen aeration process, the bitumen-air bubble attachment plays a significant role in high bitumen extraction efficiency and bitumen recovery. Hence, the effect of sodium citrate on bitumen-air bubble attachment is worth investigating. It is expected that the surface charge of air bubbles and bitumen droplets would be significantly increased in the presence of sodium citrate, suggesting low bitumen-air bubble attachment. Putting findings from a bitumen-air bubble study with the results of this study could help find the optimum dosage of sodium citrate to guarantee less slime coating and high bitumen-air bubble attachment.
2. Slime coating involves the interactions among bitumen droplets, fine clay particles and divalent ions. In this study, the interactions among bitumen droplets, calcium

chloride and sodium citrate were investigated using QCM-D in various conditions. Apart from that, the interactions among clay particles, calcium chloride and sodium citrate are worthwhile to be studied using QCM-D as well.

3. In this study, the impact of sodium citrate on the slime coating of bitumen and clays was tested in a pure solvent condition involving only calcium ions and a low background KCl concentration. However, process water used in the oil sands industry contains various multivalent metal ions, organic molecules, and anions not included in this study that may influence the performance of sodium citrate on preventing slime coating. In this way, the same measurements could be repeated using process water from the oil sands industry as a background solution.

4. Atomic force microscopy (AFM) has been used to study the interaction forces between many materials, including bitumen droplets and clay minerals. The effect of sodium citrate on the slime coating of bitumen and clays can also be examined using AFM to identify the dominant colloidal forces that prevent slime coating.

5. More adsorption tests can be conducted to further understand the role of sodium citrate on the adsorption of calcium ions on clay particle surfaces. In addition, more elements can be analyzed to more fully characterize the adsorption of cations on clay particles and the effects of sodium citrate.

6. Once the mechanism of sodium citrate on preventing slime coating has proven, more low-cost and environmental-friendly secondary processing aids may be developed to improve bitumen recovery.

References

Abou-Shakra, Fadi. (2003). Chapter 12 - Biomedical applications of inductively coupled plasma mass spectrometry (ICP-MS) as an element specific detector for chromatographic separations. In I. D. Wilson (Ed.) *Handbook of Analytical Separations* (Vol. 4, pp. 351-371). Elsevier Science B.V.

Alberta Energy Regulator. (2018). *Statistical Series 39: Alberta Mineable Oil Sands Plant Statistics, Monthly Supplement*. Retrieved from the Alberta Energy Regular website: https://www.aer.ca/documents/sts/ST39-2018.pdf.

Alberta Government (2018). *Alberta oil sands industry quarterly update (2018 Summer)*. Retrieved from the Government of Alberta website: https://open.alberta.ca/publications/2614198.

Arnold, B. J., & Aplan, F. F. (1986). The effect of clay slimes on coal flotation, part II: The role of water quality. *International Journal of Mineral Processing*, *17*(3–4), 243–260.

Bakhtiari, M.T., Harbottle, D., Curran, M., Ng, S., Spence, J., Siy, R., Liu, Q., Masliyah, J. & Xu, Z. (2015). Role of Caustic Addition in Bitumen–Clay Interactions. *Energy & Fuels*, *29(1)*, 58-69.

Banerjee, D. K. (2012). *Oil sands, heavy oil & bitumen: From recovery to refinery*. Tulsa, OK: PennWell Books.

Basu, S., Nandakumar, K., & Masliyah, J. H. (1997). On bitumen liberation from oil sands. *The Canadian Journal of Chemical Engineering*, *75*(2), 476-479.

Bergaya, F., & Lagaly, G. (2006). Chapter 1 General Introduction: Clays, Clay Minerals, and Clay Science. In F. Bergaya, B.K.G. Theng, & G. Lagaly (Eds.), *Developments in Clay Science: Handbook of Clay Science* (Vol 1., pp 1-18). Elsevier.

Bichard, J. (1987). Oil sands composition and behaviour research. *Alberta Oil Sands Technology & Research Authority (AOSTRA)*, *3*, 13–46.

Bowman, C. W. (1967). Molecular and interfacial properties of Athabasca tar sands. In *7th World Petroleum Congress*. World Petroleum Congress, Mexico City, Mexico.

Butt, H. J., & Kappl, M. (2010). *Surface and interfacial forces*. Weinheim: John Wiley & Sons, Ltd.

Carrigy, M. A., In Kramers, J. W., Canadian Society of Petroleum Geologists., & Canadian Society of Petroleum Geologists Oil Sands Symposium. (1973). *Guide to the Athabasca Oil Sands area*. Edmonton, Alberta: Alberta Research.

Chen, Q., Xu, S., Liu, Q., Masliyah, J., & Xu, Z. (2016). QCM-D study of nanoparticle interactions. *Advances in Colloid and Interface Science*, *233*, 94–114.

Cho, N., Kanazawa, K.K., Glenn, J.S. & Frank, C.W. 2007, "Employing two different quartz crystal microbalance models to study changes in viscoelastic behavior upon transformation of lipid vesicles to a bilayer on a gold surface", *Analytical Chemistry,* vol. 79, no. 18, pp. 7027-7035.

Dai, Q., & Chung, K. H. (1995). Bitumen—sand interaction in oil sand processing. *Fuel*, *74*(12), 1858–1864.

Dai, Q., & Chung, K. H. (1996). Hot water extraction process mechanism using model oil sands. *Fuel*, *75*(2), 220–226.

Das, S. K., & Butler, R. M. (1998). Mechanism of the vapor extraction process for heavy oil and bitumen. *Journal of Petroleum Science and Engineering*, *21*(1–2), 43–59.

Dékány, I. (2002). Colloid and surface properties of clays and related minerals. *Reaction Kinetics and Catalysis Letters* , *77(2)*, 393-394

Ding, X., Repka, C., Xu, Z., & Masliyah, J. (2008). Effect of Illite Clay and Divalent Cations on Bitumen Recovery. *The Canadian Journal of Chemical Engineering*, *84*(6), 643–650.

Flury, C., Afacan, A., Bakhtiari, M. T., Sjöblom, J., & Xu, Z. (2014). Effect of caustic type on

bitumen extraction from Canadian oil sands. *Energy & Fuels*, *28*(1), 431-438.

Forbes, E., Davey, K. J., & Smith, L. (2014). Decoupling rehology and slime coatings effect on the natural flotability of chalcopyrite in a clay-rich flotation pulp. *Minerals Engineering*, *56*, 136-144.

Gan, W., Crozier, B., & Liu, Q. (2009). Effect of citric acid on inhibiting hexadecane–quartz coagulation in aqueous solutions containing Ca2+, Mg2+ and Fe3+ ions. *International Journal of Mineral Processing*, *92*(1-2), 84-91.

Gan, W., & Liu, Q. (2008). Coagulation of bitumen with kaolinite in aqueous solutions containing Ca2+, Mg2+ and Fe3+: Effect of citric acid. *Journal of Colloid and Interface Science*, *324*(1–2), 85–91.

Gu, G., Sanders, R. S., Nandakumar, K., Xu, Z., & Masliyah, J. H. (2004). A novel experimental technique to study single bubble-bitumen attachment in flotation. *International Journal of Mineral Processing*, *74*(1–4), 15–29.

Hein, F. J., Marsh, R. A., & Boddy, M. J. (2008). Overview of the oil sands and carbonate bitumen of Alberta: Regional geologic framework and influence of salt-dissolution effects. *Abstracts, American Association of Petroleum Geologists*.

Hepler, L. G., & Smith, R. G. (1994). The Alberta oil sands: industrial procedures for extraction and some recent fundamental research, AOSTRA technical publication series# 14. *Alberta Oil Sands Technology and Research Authority, Edmonton, AB*.

Kasongo, T., Zhou, Z., Xu, Z., & Masliyah, J. (2000). Effect of clays and calcium ions on bitumen extraction from Athabasca oil sands using flotation. *The Canadian Journal of Chemical Engineering*, *78*(4), 674-681.

Konan, K. L., Peyratout, C., Bonnet, J. P., Smith, A., Jacquet, A., Magnoux, P., & Ayrault, P. (2007). Surface properties of kaolin and illite suspensions in concentrated calcium hydroxide

medium. *Journal of Colloid and Interface Science*, *307*(1), 101–108.

Li, H., Long, J., Xu, Z., & Masliyah, J. H. (2008). Novel polymer aids for low-grade oil sand ore processing. *Canadian Journal of Chemical Engineering*, *86*(2), 168–176.

Liu, J., Zhou, Z., Xu, Z., & Masliyah, J. (2002). Bitumen-clay interactions in aqueous media studied by zeta potential distribution measurement. *Journal of Colloid and Interface Science*, *252*(2), 409–418.

Liu, J., Xu, Z., & Masliyah, J. (2004a). Interaction between bitumen and fines in oil sands extraction system: Implication to bitumen recovery. *The Canadian Journal of Chemical Engineering*, *82*(4), 655-666.

Liu, J., Xu, Z., & Masliyah, J. (2004b). Role of fine clays in bitumen extraction from oil sands. *AIChE Journal*, *50*(8), 1917–1927.

Liu, J., Xu, Z., & Masliyah, J. (2005). Colloidal forces between bitumen surfaces in aqueous solutions measured with atomic force microscope. *Colloids and Surfaces A: Physicochemical and Engineering Aspects*, *260*(1–3), 217–228.

Long, J., & Gu, Y. J. (2015). *US 2015/0210929 A1*. Retrieved from https://pdfs.semanticscholar.org/0953/d8eeb7f38d76444fc0e3c4116cd5bdb61adb.pdf

Long, J., Li, H., Xu, Z., & Masliyah, J. H. (2006). Role of colloidal interactions in oil sand tailings treatment. *AIChE Journal*, *52*(1), 371–383.

Masliyah, J., Zhou, Z. J., Xu, Z., Czarnecki, J., & Hamza, H. (2004). Understanding water-based bitumen extraction from Athabasca oil sands. *The Canadian Journal of Chemical Engineering*, *82*(4), 628-654.

Masliyah, J.H. & Czarnecki, Jan & Xu, Zhenghe. (2011). *Handbook on theory and practice of bitumen recovery from Athabasca oil sands - Volume 1: Theoretical basis* (pp. 115-116). Alberta: Kingsley Knowledge Publishing.

Nageswaran, G., Choudhary, Y. S., & Jagannathan, S. (2017). Chapter 8 - Inductively Coupled Plasma Mass Spectrometry. In S. Thomas, R. Thomas, A. K. Zachariah, & R. K. Mishra (Eds.) *Spectroscopic Methods for Nanomaterials Characterization* (pp. 163–194). Elsevier

Najafi, A., Xu, Z. & Masliyah, J. (2008). Measurement of Sliding Velocity and Induction Time of a Single Micro-Bubble Under an Inclined Collector Surface. *Can J Chem Eng,* 86(6), 1001-1010.

Salopek, B., Krasic, D., & Filipovic, S. (1992). Measurement and application of zeta-potential. *Rudarsko-geolosko-naftni zbornik*, *4*(1), 147.

Sauerbrey, G. (1959). Verwendung von Schwingquarzen zur Wägung dünner Schichten und zur Mikrowägung. *Zeitschrift Für Physik*, *155*(2), 206–222.

Schramm, L. L. (2006). *Emulsions, foams, and suspensions: fundamentals and applications*. John Wiley & Sons.

Schramm, L. L. (2000). *Surfactants: fundamentals and applications in the petroleum industry*. Cambridge University Press.

Singh, A. K. (2016). Chapter 4 - Experimental Methodologies for the Characterization of Nanoparticles. In A. K. Singh (Ed.) *Engineered Nanoparticles* (pp. 125-170). Boston, MA: Academic Press

Strausz, O. P. (1989). Bitumen and heavy oil chemistry. *AOSTRA Technical Handbook on Oil Sands, Bitumens and Heavy Oils*, 33–73.

Takamura, K. (1982). Microscopic structure of athabasca oil sand. *The Canadian Journal of Chemical Engineering*, *60*(4), 538–545.

Valiño, V., San Román, M. F., Ibáñez, R., Benito, J. M., Escudero, I., & Ortiz, I. (2014). Accurate determination of key surface properties that determine the efficient separation of bovine milk BSA and LF proteins. *Separation and Purification Technology*, *135*, 145–157.

Vashishtha, S., & Maheshwari, U. (2014). Oil sands processing: An unconventional source of

synthetic crude oil. *17th Topical on Refinery Processing 2014 - Topical Conference at the 2014 AIChE Spring Meeting and 10th Global Congress on Process Safety*, (February), 2–3.

Wallace, D., Henry, D., & Takamura, K. (1989). A physical chemical explanation for deterioration in the hot water processability of athabasca oil sand due to aging. *Fuel Science and Technology International*, *7*(5–6), 699–725.

Wallwork, V., Xu, Z., & Masliyah, J. (2008). Processibility of Athabasca Oil Sand Using a Laboratory Hydrotransport Extraction System (LHES). *The Canadian Journal of Chemical Engineering*, *82*(4), 687–695.

Wik, S., Sparks, B. D., Ng, S., Tu, Y., Li, Z., Chung, K. H., & Kotlyar, L. S. (2008). Effect of process water chemistry and particulate mineralogy on model oilsands separation using a warm slurry extraction process simulation. *Fuel*, *87*(7), 1394–1412.

Xiang, B., Liu, Q., & Long, J. (2018). Probing Bitumen Liberation by a Quartz Crystal Microbalance with Dissipation. *Energy and Fuels*, *32*(7), 7451–7457.

Xu, G., D., Dopico, P., Johnson, S., Hines, J., & Kennedy, D. (2012). Clay Binder Enhanced Extraction of Bitumen from Canadian Oil Sand. *2012 SME Annual Meeting and Exhibit 2012, SME 2012, Meeting Preprints*.

Zhao, H., Dang-Vu, T., Long, J., Xu, Z., & Masliyah, J. H. (2009). Role of bicarbonate ions in oil sands extraction systems with a poor processing ore. *Journal of Dispersion Science and Technology*, *30*(6), 809–822.

Zhao, H., Long, J., Masliyah, J. H., & Xu, Z. (2006). Effect of divalent cations and surfactants on silica-bitumen interactions. *Industrial and Engineering Chemistry Research*, *45*(22), 7482–7490.